Published in Applied Energy with doi: 10.1016/j.apenergy.2025.126251

Robust Dynamic Charging Price in PV-assisted Charging Stations

Marcos Tostado-Véliz[1,*], Hany M. Hasanien[2,3], Paul Arévalo[4], Francisco Jurado[1]

1. Department of Electrical Engineering, University of Jaén, 23700 Linares, Spain (e-mail: mtostado@ujaen.es (M.T.-V.), fjurado@ujaen.es (F.J.)).
2. Electrical Power and Machines Department, Faculty of Engineering, Ain Shams University, Cairo 11517, Egypt (e-mail: hanyhasanien@ieee.org).
3. Faculty of Engineering and Technology, Future University in Egypt, Cairo 11835, Egypt
4. Department of Electrical Engineering, Electronics and Telecommunications (DEET), Faculty of Engineering, University of Cuenca, Balzay Campus, Cuenca 010107, Ecuador (e-mail: paul.arevaloc@ucuenca.edu.ec).

* Correspondence: mtostado@ujaen.es

Abstract. With the increasing number of electric vehicles on road, the deployment of sufficient public charging infrastructures has become critical. To encourage the installation of new public charging points, such infrastructures need to be economically viable and profitable. In this regard, exploring economic activities within charging infrastructures has become a key topic to ensure the long-term financial sustainability of charging installations. In line with this objective, this paper develops a new robust methodology to setting dynamic charging prices in charging stations. Unlike to conventional charging prices based on flat tariffs, dynamic pricing strategies can follow wholesale electricity prices, potentially setting low prices and therefore displacing the fleet from domestic to public charging. The new proposal renders as a game-theoretical max-min bi-level optimization problem. To address the initial complexity of the formulation, a tailored solution algorithm is developed, which allows accessing to robust solutions efficiently. An adaptive robust modelling of uncertainties is proposed, based on intervals, which allows representing uncertainties as box-constrained variables. Moreover, this paper contributes with a new data-driven approach to determine limits on uncertainties based on bootstrapping. The new solution strategy is validated on a benchmark large-scale charging station installing a photovoltaic facility. Additionally, the effect of the risk level and photovoltaic size on final results is evaluated. In addition, the effectiveness of the charging pricing strategy is assessed, along with the influence of uncertainties on the final results.

Keywords. Bootstrapping; Fast charging; Electric vehicles; Robust optimization

1 – Introduction

1.1 – Context and motivation

Electric vehicle (EV) sales were a 35% higher in 2023 compared to 2022, thus bringing up to 40 million of electric cars on the road (18% of the total) worldwide [1]. The extraordinary increase in EV sales during the last decade has been accompanied by a significant deployment of charging infrastructures, reaching near 40 million of private/public charging points in 2023 [1]. However, only a small portion (about 3% of the total) are public infrastructures equipped with fast chargers. The clear lack of public fast chargers may suppose a barrier for the widely adoption of electric mobility options. Indeed, most of the existing domestic charging points require many hours to fully charge an average commercial EV, thus limiting the capacity of EVs to complete long-travel distances due to lack of fast charging infrastructures on the road [2].

In order to increase the number of EVs on the road and definitely displace pollutant mobility technologies, it is essential to significantly expand the number of public fast charging infrastructures within the next few years. To promote the installation of new charging stations, such infrastructures must be economically attractive and profitable. Consequently, public authorities have launched different initiatives, primarily focused on subsidizing the cost of installing public and private charging points [3, 4]. However, solely subsidizing its installation appears insufficient to guarantee long-term viability of public charging points. Therefore, new economic activities should be explored to ensure that fast public chargers remain financially sustainable, with short payback periods [5].

1.2 – Dynamic charging price, why?

Currently, public charging stations implement fixed prices for charging, thus providing fair and stable pricing signals to EV users. However, these charging prices remain high in comparison to retail electricity rates. As a result, EV users are still hesitant to widely use public charging infrastructures, preferring the use of domestic charging points [6]. Changing to dynamic pricing strategy, aligned with dynamic wholesale electricity signals, could reduce charging prices but still ensuring the profitability of public infrastructures while attracting a growing number of EV users. However, developing such a dynamic pricing strategy is a complex task that requires the use of advanced computational tools to identify the optimal pricing and assess the implications of its implementation. This paper addresses this issue.

1.3 – Dynamic charging price, a literature review

Lu et al [7] propose a real-time-price (RTP) strategy for domestic chargers with the aim of maximizing the utility of users while minimizing the cost of the whole generation mix, but neglecting further demand response from charging demand. In [8], the EV fleet is modelled using graph theory and Monte Carlo simulation, with the objective of determining its charging demand. This information then serves as input for a two-stage optimization model, in whose first stage the cost of charging is minimized thus determining the optimal pricing strategy, while in the second stage the operation of the distribution network is considered to ensure its voltage stability. Zhou et al [9] develop a dynamic charging price model taking into account the traffic network. The resulting pricing seeks for minimizing the travelling time of EVs by determining the zonal charging price using algorithmics an logic decision chain rather than optimization.

An optimal charging price strategy is proposed in [10] with a bi-objective. On the one hand, the peak-to-average ratio of the distribution network is minimized. On the other hand, the determined pricing strategy seeks for utilizing on-board batteries more profusely, encouraging users to charge when the state-of-charge (SoC) is beyond a threshold. This arrangement casts as a complex optimization model that is solved using metaheuristics. Feng and Czarkowski [11] propose a locational charging price to allow EV users to choose among different charging stations (CSs), which are considered strategic agents. The model is then optimized seeking for Nash

equilibrium. However, its reachability is not ensured as metaheuristics are used for solving the model. In [12], a non-cooperative game framework is developed, for optimal management of distribution networks in the presence of EVs. The objective is alleviating network congestion by dynamically adjusting charging prices. Thereby, EVs can choose where to charge based on locational pricing. Sheng et al [13] develop a Stackelberg game framework for coordinated pricing of coupled traffic and power networks, with special focus on the value of information sharing between systems.

Vuelvas et al [14] develop a bi-level optimization model, in which the CS acts as the leader at the upper-level, whereas the parking lot (PL) plays as the follower in the lower one. This way, the optimization model results in a Stackelberg game approach, by which charging prices are determined in the Nash sense, allowing EVs to adjust their charging schedule according to prices. A multi-strategic firm competitive charging pricing is developed in [15]. Specifically, this proposal casts as a multi-leader single-follower optimization model, where different CSs compete in prices for getting clients. This way, EV users can choose the station where they will charge. It results in a complex optimization model which is eventually solved using deep reinforcement learning, which questions the optimality of the final pricing policy. Similarly, charging prices are determined in [16] by solving a non-cooperative game approach. However, this work considers a strategic alliance among CSs which is equivalent to consider a unique charging provider. In this case, the complexity of the mathematical model is circumvented employing metaheuristics, which do not ensure the global optimum solution and, in consequence, the reachability of the Nash equilibrium point. Liu et al [17] concern about the strong synergies between power and traffic networks. Specifically, a collaborative routing and charging scheduling model is proposed, resulting a bi-layer methodology where the power and traffic-related problems are solved separately.

In [18], a pricing strategy is developed by which EV users can select the most adequate charging point and price menu. In this sense, this proposal aims at extracting privacy features of users in order to best determine the pricing strategy to follow. To this end, a Stackelberg game approach is proposed, in which the CS acts as leader and EVs as followers. Li et al [19] propose a learning-based algorithm for charging price determination in integrated systems. The main novelty of this work lies in the inclusion of three different agents, namely the traffic network, the power system and the microgrid sub-network encompassing hydrogen refilling stations, local storage systems and photovoltaics (PVs). In this regard, each agent aims at minimizing its own cost while seeking for equilibrium in a learning environment. In [20], two types of game frameworks are compared for charging price determination. On the one hand, the conventional non-cooperative games based on Stackelberg theory, which are considered as a benchmark. In contrast, cooperative bargaining games are also considered, giving some tricks to linearize their objectives and constraints.

Gao et al [21] investigate how to incorporate distribution locational marginal prices into charging pricing policy. To this end, a collaborative approach is proposed, by which CSs in a distribution network forms a strategic alliance. The pricing model is then formed by the marginal price and a free term accounting for the profit of the station. Sharing rules based on Shapley value are envisioned to share the profit in a fair manner. An optimal pricing strategy is proposed for parking clusters in [22]. This approach allows further demand response from EV users, calculating optimal charging/discharging prices enabling vehicle-to-grid technologies. Interval-guided uncertainties are considered, assuming that energy margins available in the parking can be impacted by unpredictable behaviour of drivers. In [23], a two-stage game theoretical model is proposed for price setting in coupled traffic, information and power environments. More specifically, the power network is divided into electrical and urban areas in the first stage, while the optimal pricing strategy is decided in the second stage following non-cooperative game assumptions. Unsupervised learning has been applied for coordinating charging loads and traffic flows in coupled traffic-power networks in [24]. The developed technique transforms the

optimization model into an unconstrained nonlinear optimization framework, whose features are learned using an unsupervised surrogate model. For the sake of simplicity, Table 1 summarizes the main features of the studied literature.

Table 1 - Summary of the relevant literature

Ref.	EV response				Uncert.	Renew.
	Where	When	How much	Disch.		
[10]						
[19]						✓
[11, 23]	✓					
[9]	✓					✓
[14]	✓	✓				
[7]		✓	✓			
[22]		✓		✓	✓	
This	✓	✓	✓	✓	✓	✓

1.4 – Research gaps

In the light of the literature survey above, which is summarized in Table 1, it is clear that most of the existing works raise game theoretical frameworks to derive dynamic charging prices. This approach effectively captures users' interests and, in consequence, prices are established through equilibrium instead of seeking for individual profit of the charging infrastructures. Nevertheless, in most of the reviewed works, the response capacity of EVs is often limited. In most of references [11, 12, 15, 16, 20, 21, 23], EVs can choose where to charge solely, while other capabilities are neglected. In other references, EVs a more widely flexibility is enabled, allowing to choose when [14], and how much energy [7] is charged. However, only reference [22] considers vehicle-to-grid capability, enabling on-board batteries to be discharged. Considering a wide response of vehicles allows assessing better the impact of dynamic charging prices in their response. In consequence, further research is required to assess the impact of dynamic charging prices not only in charging schedules, but also in discharging routines.

On the other hand, the majority of the reviewed references assume deterministic conditions, which is a strong assumption in EV-related problems due to the random behaviour of drivers. Certainly, some references consider probabilistic models to derive the drivers' behaviour. Nevertheless, these approaches are only employed to estimate the charging demand, typically. This data serves as input of the optimization problem, which does not pay attention to the risk associated to uncertainties. Reference [22] appears to be, to the best of our knowledge, the sole exception. Nonetheless, the model proposed in this reference does not explicitly raises risk-averse or risk-seeker optimization strategies. Instead, two different strategies are proposed on the basis evolution of uncertainties. In other words, the model in [22] necessitates prior knowledge on the impact of uncertainties on final results, thus rendering as a case-dependent approach. In this sense, there is a clear lack of uncertainty modelling in dynamic charging price models, especially related to modelling the driving behaviour of users.

Finally, only some few works consider CSs equipped with renewable onsite generators. Note that the inclusion of local renewable generation may have a significant impact on charging prices, enabling self-sufficiency. Indeed, the availability of renewable generation might allow reducing charging prices, thus displacing charging demand to central hours. Thereby, the CS might inhibit itself from wholesale prices from the main grid, thus leading to a decoupling effect between the grid and station prices. Furthermore, discharging scheduling might be significantly impacted by renewable penetration. It is worth noting that renewable generation introduces further uncertainties that need to be modelled and assessed properly.

1.5 – Contributions and paper organization

The contributions of this paper are twofold:

- Developing a Stackelberg game approach for setting charging prices in PV-assisted CSs. The key innovation lies in the integration of adaptive robust programming within the bi-level Stackelberg framework. To achieve this, a customized algorithm is designed, capable of effectively determining the worst-case scenarios of uncertainties and generating robust solutions. Additionally, several uncertainties are modelled and assessed, including SoC limits, PV potential, wholesale prices, and maximum charging power.
- Unlike [22], the proposed approach inherently seeks robust solutions, meaning that prior knowledge of the impact of uncertainties is not required. In this regard, an interval-guided modeling of uncertainties is employed, in line with [22]. However, while the existing reference does not provide details on how to determine the limits of uncertainties, this paper introduces a novel data-driven methodology based on bootstrapping [25], which allows for determining the bounds of uncertainties when modelled as box-constrained variables.

As shown in Table 1, this paper contributes to the body of knowledge with a novel methodology that offers improvements over others, primarily in the robust solution algorithm, EVs response and uncertainty modelling. It is important to highlight that the proposed methodology focuses mainly on setting prices in middle and long-term horizons. This assumption aligns with real cases, where decision-makers and clients typically seek stable prices. In this sense, long-term variation of uncertainties can be more effectively captured using robust techniques, as opposed to others such as stochastic programming [26].

Accordingly, the uncertainty modelling approach adopted in this study is consistent with other robust optimization frameworks presented in the literature, which do not require prior specification of the impact of uncertainties. It is important to note that robust optimization has previously been applied to traffic-related problems [27]. However, the study in [27] focuses on the robust formulation for optimal network expansion planning and does not address the issue of charging price determination. Specifically, this work adopts the perspective of the distribution system operator, whereas the present work centres on the role of the charging service provider, particularly at the level of individual charging stations. Furthermore, the model in [27] is solved using a bi-level formulation tailored to expansion planning, which is not directly applicable to Stackelberg game-based approaches as employed in this paper. As a result, the methodology used in [27] does not permit the direct computation of charging prices within the robust framework.

In the rest of this paper, Section 2 provides the necessary background and states the problem. Section 3 describes the price-setting formulation as a bi-level Stackelberg game framework. Section 4 explains the main contributions of the paper, including the developed robust optimization algorithm as well as the bootstrapping methodology to calculate the limits of the uncertainty set. Section 5 presents a case study with results to validate the model. Finally, the paper is concluded with Section 6.

2 – Preliminaries

2.1 – Notation

The notation employed throughout this paper is detailed below, where ‘pu’ refers to per-unit.

Indices (sets)	
t ($\mathcal{T}$)	Time $t \in \{0,1,2,\dots,T\}$
v ($\mathcal{V}_t$)	Vehicles plugged at time t
$\mathcal{V}_t^{\rightarrow}$	Vehicles leaving the parking at time t
ω (Ω)	Uncertain parameters
Superscripts	

CS	Charging station
PL	Parking lot
c/d	Charging/discharging
im/ex	Importing/exporting
B	Batteries
G	Grid
PV	Photovoltaic
$\underline{(\cdot)}/\overline{(\cdot)}$	Minimum/maximum value of a variable or parameter
$\tilde{(\cdot)}$	Given value
Parameters	
$\Delta_{\omega}^{\downarrow}/\Delta_{\omega}^{\uparrow}$	Lower/upper bandwidth for representing the uncertain parameter via intervals (€/MWh or MWh or MW)
$\mathbb{E}[\cdot]$	Expected value of an uncertain parameter
α	Risk level (pu)
η	Efficiency (pu)
d	Depth-of-discharge (pu)
C	Replacement cost (€/MWh)
L	Lifecycle (cycles)
ρ	Degradation cost (€/MWh)
W	Wholesale electricity price (€/MWh)
σ^{ex}	Discount in exporting price (pu)
Bootstrapping	
θ	Vector of input data formed by Θ elements
$\theta_k^{w_n}$	k^{th} element of the sub-sample of the input data vector determined by the indexes collected in the vector w_n
n (N)	Bootstrap sample (total number of bootstrap samples)
K	Size of bootstrap samples
$\text{randi}(a, b)$	Generates b integer random numbers between 1 and a
$\underline{\theta}/\overline{\theta}$	Estimated lower/upper bounds for the input data
$\mathbb{Q}_q[\cdot]$	Yields the q^{th} percentile of a sample
Decision variables (primal)	
p	Power (MW)
SoC	State-of-charge (MWh)
λ	Charging price (€/MWh)
Decision variables (dual)	
ϕ	Dual variables linked to equality constraints (€/MWh)
$\underline{\mu}/\overline{\mu}$	Dual variables linked to inequality constraints (€/MWh)

2.2 – Description of the system under study

For the sake of simplicity, Fig. 1 sketches the charging system under study and summarizes some of the mathematical notation employed in this paper. We consider the case in which a number of EVs intends to charge their on-board batteries before unplugging. Rather than being managed individually, we assume that the charging/discharging schedules of all the vehicles are coordinated by a central agent called PL. This arrangement is consistent with others proposed in the literature [14, 22], and is therefore assumed to be implementable in real-life cases.

Furthermore, The CS (eventually managed by the station operator) sets charging prices in advance to meet local charging demand, facing the challenge of establishing competitive prices in order to attract clients in the PL.

The station is equipped with a PV system, which is managed by the station operator and can supply the local charging demand in the event of sufficient renewable potential. Additionally, the station is directly connected to an upscale grid (transmission system), allowing it to exchange energy at wholesale electricity prices. On the other hand, the PL can choose whether charging or discharging in the station or looking for other options in the grid. Such decision will be mainly motivated on pricing signals received from the charging infrastructure or directly from the grid. Thus, the station operator will compete in prices in order to maximize the number of vehicles that charge in the station. Moreover, EVs can discharge on-board batteries and be paid under dynamic charging prices.

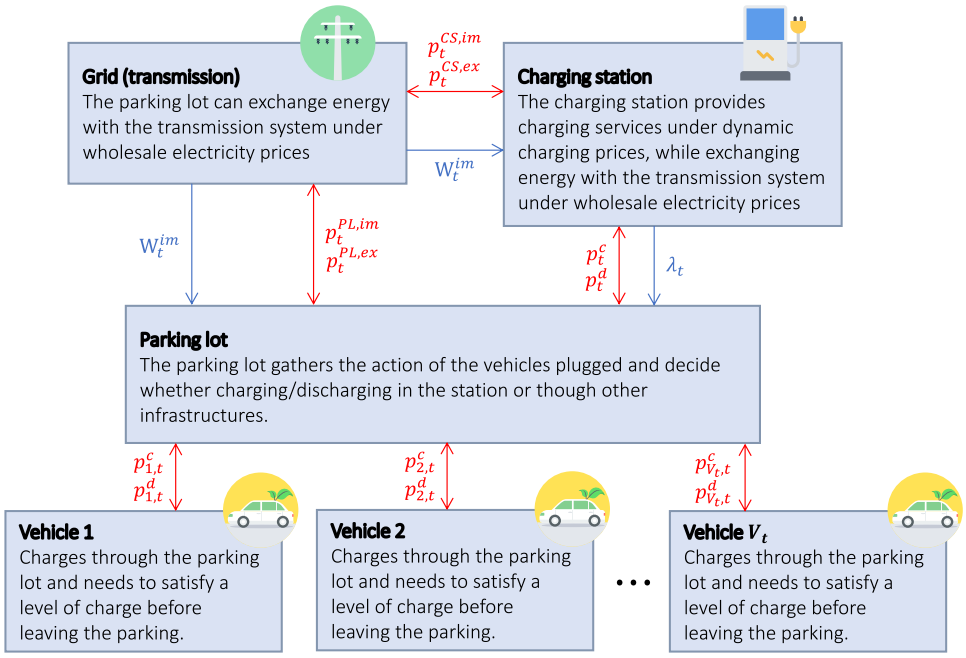

Fig. 1 – Sketch of the considered charging system

2.3 – Assumptions

The Stackelberg model outlined in Fig. 1 and further developed in the subsequent mathematical formulation assumes the following:

- EV owners act as passive players, only interested on charging their EVs before unplugging. In this regard, it is assumed that EV owners delegate their charging/discharging schedules to the PL, which oversees the control of all the vehicles that are plugged-in.
- The PL can charge/discharge EVs either in the CS under dynamic charging prices or directly from the grid at wholesale rates. Hence, it is assumed that alternative charging options, such as domestic chargers, are integrated within the grid agent, which serves as an external power supplier.
- The PL role is limited to coordinating the action of all the EVs in order to simplify their coordination and protect privacy. In this sense, the PL is not focused on maximizing its profit but instead acts as a budget-balanced player, similar to the community manager in [28].

2.4 – Problem statement

The charging price-setting problem described above aligns with the principles of Stackelberg game models. Indeed, Stackelberg games involve the coexistence of a leader and one or more

followers [29]. In the game, the leader decides first and wait for the followers' reaction. To address the charging price-setting problem, we adopt a Stackelberg game framework in which the CS acts as the leader, deciding on charging prices, while the users in the lot play the role of followers, adjusting their charging/discharging schedules and preferences in response. Furthermore, we will incorporate the effect of uncertainties. Specifically, we will develop a robust programming approach that facilitates decision-making under worst-case realization of uncertainties. This problem can be mathematically stated, as follows:

$$\max_{\Omega} \min_{\lambda_t, x^{CS}} F^{CS} \tag{1a}$$

Subject to:

$$g^{\omega}(\Omega) \leq 0 \tag{1b}$$

Subject to:

$$h^{CS}(x^{CS}, x^{PL}, \Omega^{CS}) = 0 \tag{1c}$$
$$g^{CS}(x^{CS}, \Omega^{CS}) \leq 0 \tag{1d}$$
$$x^{PL} \in \underset{x^{PL}}{\operatorname{argmin}}\{F^{PL}: h^{PL}(x^{PL}, \Omega^{PL}) = 0, g^{PL}(x^{PL}, \Omega^{PL}) \leq 0\} \tag{1e}$$

Problem (1) states as a nested max-min optimization model. In the outer problem, the station cost function (F^{CS}) is maximized thus leading to the worst-case realization of uncertainties ($\Omega = \Omega^{CS} \cup \Omega^{PL}$). In the inner problem, the station operator decides on charging prices (λ_t) and own variables ($x^{CS} = \left[p_t^{CS,im}, p_t^{CS,ex}, p_t^{PV}\right]$) to minimize the station cost. The inner problem is constrained by the equality and inequality constraints of the station (1c) and (1d), which corresponds with equations (18b) and (18c)-(18f), respectively. The outer problem is also constrained by the inner problem (1e), in which the PL reacts to charging prices decided on the upper-level by adjusting their own decision variables ($x^{PL} = \left[p_t^{PL,im}, p_t^{PL,ex}, p_t^{PL,c}, p_t^{PL,d}, SoC_t^{PL}\right]$) in order to minimize the charging cost (F^{PL}) under own constraints. Moreover, different sources of uncertainties are related to outer and inner problems, denoted by the sets Ω^{CS} and Ω^{PL}, respectively. Such uncertainties can appear in equality and inequality constraints and are modelled in (1b), which is further described in (5).

Direct solution of (1) in present form supposes a challenge due to the coexistence of maximization and minimization problems, as well as the lower-level problem (1e) appearing as a constraint. While robust programming and bi-level problems can be effectively solved by deriving the 1st-order optimality conditions of the inner or lower-level problems [27, 30, 31], simultaneously addressing both approaches supposes a challenge. In Section 4, we will develop a tailored algorithm to address this issue.

2.5 – Sources of uncertainty

The mathematical formulation explained in Section 3 assumes that all the input parameters take deterministic values, and therefore, uncertainties are not further modelled. Nonetheless, this is a strong assumption, as the actual realization of many parameters remains unknown, even over short-time periods. In particular, we consider the following sources of uncertainties:

- The number of vehicles plugged any time instant is inherently uncertain, as users generally exhibit random driving behaviours [32]. Thus, the uncertain number of plugged-in vehicles impacts on the SoC and charging/discharging limits, as these parameters are directly dependent on the number of vehicles parked.
- Although PV generation can be estimated day-ahead with acceptable accuracy, its long-term (panels degradation) and seasonal features (summer, winter) need to be considered in price-setting problems.

- Similarly, next-day wholesale electricity prices can be estimated with acceptable accuracy, but they are strongly affected by long-term uncontrollable features and seasonal trends.

In conclusion, although some uncertain parameters might be forecasted over short-time horizons (e.g. 24 h in advance), their long-term variation needs to be implicitly modelled in the price-setting problem. Note that station operators are keen to set stable prices in the middle and long-term horizon typically (e.g. 1 year), and as such, these long-term uncertainty features need to be considered. Nevertheless, the proposed methodology could still be applied in day-ahead tools without major modifications.

Particularly, the considered uncertainties can be classified into those that directly impact to the station operation, and the others that are directly related with the PL. In this sense, we split the set Ω into two subsets, each collecting uncertainties in the CS and PL, as follows:

$$\Omega^{CS} \triangleq \left[\mathrm{W}_t^{im}, \overline{p}_t^{PV}\right] \tag{2}$$

$$\Omega^{PL} \triangleq \left[\underline{SoC}_t^{PL}, \overline{SoC}_t^{PL}, \overline{p}_t^{PL}\right] \tag{3}$$

It is noteworthy that the wholesale electricity price affects both, the CS and PL. However, this parameter has been included solely in the CS subset. This is because the CS first observes wholesale prices and adjusts charging prices in response. Afterwards, the PL reacts choosing when, how much and where to charge or discharge. This hierarchical sequence reveals that the CS has the ability to react to electricity prices, whereas the PL reacts to the charging prices instead. Thus, the PL is necessarily subordinated to the actions of the station, in line with the game theoretical model described in previous subsections.

2.6 – Uncertainty modelling

A variety of uncertainty representations have been studied in the literature, encompassing approaches such as stochastic or robust programming. Stochastic optimization requires perfect knowledge on the probability distribution of uncertainties. However, when such distribution is unknown or simply desire to ensure that the solution attained is safe across a range of possible realizations, robust optimization is preferred [33]. In the problem concerned in this paper, it is assumed that an agent, namely the station operator, is intended to set dynamic prices to ensure economic performance even for worst-case realization of uncertainties. Moreover, while probability distributions have been widely studied for PV potential or electricity prices, other sources of uncertainty are difficultly representable using scenarios such as SoC bounds in the PL.

By the reasons above, robust optimization has been employed in this paper instead of other approaches. A proper uncertainty modelling is key on robust optimization models. In this paper, we adopt an interval modelling of uncertainties, which has been successfully applied in other related problems [32]. Let us consider the uncertain parameter ω, which is modelled as a box-constrained variable, allowing them to vary on a range delimited by established bounds, as said (4).

$$\omega \in \left[\underline{\omega}, \overline{\omega}\right]; \forall \omega \in \Omega \tag{4}$$

The domain of ω is then described by its expected value and upper/lower bandwidths, as depicted in Fig. 2. Therefore, the box constraint (4) can be rewritten in the function of bandwidths, as follows:

$$\mathbb{E}[\omega] - \alpha\Delta_\omega^{\downarrow} \leq \omega \leq \mathbb{E}[\omega] + \alpha\Delta_\omega^{\uparrow}; \forall \omega \in \Omega \tag{5}$$

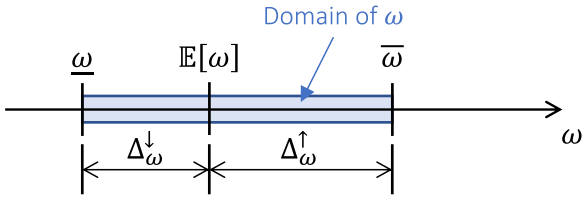

Fig. 2 – Interval modelling of the uncertain parameter ω

Eq. (5) is parameterized by the risk level $0 \leq \alpha \leq 1$, which limits the effective domain of ω. Indeed, if $\alpha = 1$, all the range described by (4) is considered and therefore ω could take any value on its original domain. In contrast, the problem becomes deterministic for $\alpha = 0$ as ω is enforced to take its expected value according to (5). In this way, the risk level allows to tune the level of risk assumed by the decision-maker. Actually, more conservative solutions will be calculated for higher values of α, while reducing it will observe the opposite effect. This adoption makes the developed robust solution adaptive and therefore more easily implementable in industrial tools.

3 – Mathematical models

3.1 – PL modelling

3.1.1 – Vehicle modelling

Each vehicle in the PL can charge/discharge on-board batteries controlling its SoC, which is given by:

$$SoC_{v,t} = SoC_{v,t-1} + \left(p_{v,t}^{c} + p_{v,t}^{im}\right)\eta_{v}^{B,c} - \left(p_{v,t}^{d} + p_{v,t}^{ex}\right)/\eta_{v}^{B,d};\ \forall v \in \mathcal{V}_t \wedge t \in \mathcal{T}\backslash\{1\} \quad (6)$$

As seen, (6) considers that vehicles can charge in the station or directly with other stations or infrastructures. The power that each vehicle can exchange is limited by the rated power of the charger or the own vehicle, as said (7). Moreover, the SoC of the vehicle is limited by the capacity of on-board batteries and its depth-of-discharge by (8).

$$0 \leq p_{v,t}^{c}, p_{v,t}^{d}, p_{v,t}^{im}, p_{v,t}^{ex} \leq \overline{p}_{v};\ \forall v \in \mathcal{V}_t \wedge t \in \mathcal{T} \quad (7)$$

$$(1 - d_{v}^{B})\overline{SoC}_{v} \leq SoC_{v,t} \leq \overline{SoC}_{v};\ \forall v \in \mathcal{V}_t \wedge t \in \mathcal{T} \quad (8)$$

3.1.2 – Aggregated modelling

The PL collectivizes the charging/discharging scheduling of all the vehicles plugged. This approach enables modelling the problem using an aggregated model rather than specifically modelling individual features. Moreover, this aggregated modelling offers the advantage of maintaining the model computationally tractable while safeguarding the privacy of owners, who share confidential information with the PL (which acts a budget-balanced agent) instead with the CS [34]. Indeed, modelling aggregated profiles increments the level of uncertainty, for which the robust approach described in Section 4 results of practical interest.

In this model, the maximum energy that can be stored in the parking is limited by the capacity of all the vehicles plugged, as follows:

$$\overline{SoC}_{t}^{PL} = \sum_{v \in \mathcal{V}_t} \overline{SoC}_{v};\ \forall t \in \mathcal{T} \quad (9)$$

Any time instant, there must be sufficient energy stored in the parking to satisfy charging requirements of those vehicles that are leaving the parking, as said (10).

$$\underline{SoC}_{t}^{PL} = \sum_{v \in \mathcal{V}_t^{\rightarrow}} \overline{SoC}_{v};\ \forall t \in \mathcal{T} \quad (10)$$

Total power exchanged by vehicles can be aggregated by simply summing up the power of all the vehicles, as said (11) and (12). These aggregated powers allow calculating the aggregated SoC in the lot according to (13).

$$p_t^{PL,c} = \sum_{v\in\mathcal{V}_t} p_{v,t}^{c}\,, p_t^{PL,d} = \sum_{v\in\mathcal{V}_t} p_{v,t}^{d}\,;\ \forall t \in \mathcal{T} \tag{11}$$

$$p_t^{PL,im} = \sum_{v\in\mathcal{V}_t} p_{v,t}^{im}\,, p_t^{PL,ex} = \sum_{v\in\mathcal{V}_t} p_{v,t}^{ex}\,;\ \forall t \in \mathcal{T} \tag{12}$$

$$SoC_t^{PL} = SoC_{t-1}^{PL} + \left(p_t^{PL,c} + p_t^{PL,im}\right)\tilde{\eta}^{B,c} - \left(p_t^{PL,d} + p_t^{PL,ex}\right)/\tilde{\eta}^{B,d};\ \forall t \in \mathcal{T}\backslash\{1\} \tag{13}$$

Equation (13) assumes the same efficiency for all the vehicles in the lot. Note that this is a reasonable assumption as commercial EVs typically install Li-ion batteries, whose efficiency is in the range 90-95 %, usually [35]. Thereby, the model adopts an average efficiency without incurring in significant errors. Power limits can be aggregated similarly, as follows:

$$0 \le p_t^{PL,c}, p_t^{PL,d}, p_t^{PL,im}, p_t^{PL,ex} \le \sum_{v\in\mathcal{V}_t} \overline{p}_v = \overline{p}_t^{PL};\ \forall t \in \mathcal{T} \tag{14}$$

3.1.3 – Battery degradation

Excessive charging-discharging cycles may degrade batteries due to cyclic aging [35]. This degradation should be considered in the developed operational model to account for the cost of battery deterioration and prevent over-using on-board batteries. Although it has been demonstrated that cyclic aging is a quadratic function of the depth-of-discharge [36], several studies have proposed well-behaved linear approximations for economic purposes [37, 38]. In particular, we adopt the model presented in [37], which estimates the degradation cost as a function of different battery parameters and the total power exchanged, as follows:

$$D_{v,t}\left(p_{v,t}^{c}, p_{v,t}^{d}, p_{v,t}^{im}, p_{v,t}^{ex}\right) = \frac{C_v^B p_{v,t}^B}{2L_v^B \overline{SoC}_v d_v^B \eta_v^{B,c} \eta_v^{B,d}};\ \forall v \in \mathcal{V}_t \wedge t \in \mathcal{T} \tag{15}$$

where $p_{v,t}^B = p_{v,t}^c + p_{v,t}^d + p_{v,t}^{im} + p_{v,t}^{ex}$. The depth-of-discharge in (15) is defined as the relative difference between the maximum and minimum capacity of batteries [36]. In commercial EVs, the depth-of-discharge is typically set below 80 % to avoid fast degradation of on-board batteries [39]. Following the aggregated model proposed in Section 3.1.2, we consider the total degradation cost in the lot, as follows:

$$D_t^{PL} = \sum_{v\in\mathcal{V}_t} \rho_v^B p_{v,t}^B\,;\ \forall t \in \mathcal{T} \tag{16}$$

Note that determining the degradation cost of each vehicle is a challenge, especially when the characteristics of vehicles are unknown. In this sense, we propose deriving ρ_v^B through statistical analysis. By considering different features of commercial EVs, a sufficiently large sample can be generated. Subsequently, the value of ρ_v^B can be calculated as the mean value of the distribution obtained or, if robust solutions are looked for, a reasonably high percentile in the density function (e.g. 97.5%) may be selected.

3.1.4 – Operational model of the PL

The PL can choose when, how much (within SoC limits) and where to charge/discharge in order to minimize its cost. As previously discussed, an aggregated model of the plugged-in EVs is considered, meaning that individual features are not explicitly included but aggregated profiles are used, thus simplifying the coordination and management of the vehicles in the lot. Following these premises, the operational PL model can be written as:

$$\min_{x^{PL}} F^{PL} = \sum_{t\in\mathcal{T}}\left\{\left(p_t^{PL,c} - p_t^{PL,d}\right)\lambda_t + \mathrm{W}_t^{im}\left(p_t^{PL,im} - \sigma^{ex} p_t^{PL,ex}\right) + D_t^{PL}\right\} \tag{17a}$$

Subject to:

$$SoC_t^{PL} = SoC_{t-1}^{PL} + \left(p_t^{PL,c} + p_t^{PL,im}\right)\tilde{\eta}^{B,c} - \left(p_t^{PL,d} + p_t^{PL,ex}\right)/\tilde{\eta}^{B,d} : \langle \phi_t^{SoC}\rangle;\ \forall t \in \mathcal{T}\backslash\{1\} \tag{17b}$$

$$SoC_{(t=1)}^{PL} = \left(p_{(t=1)}^{PL,c} + p_{(t=1)}^{PL,im}\right)\tilde{\eta}^{B,c} - \left(p_{(t=1)}^{PL,d} + p_{(t=1)}^{PL,ex}\right)/\tilde{\eta}^{B,d} : \langle \phi_{(t=1)}^{SoC}\rangle \tag{17c}$$

$$\underline{SoC}_t^{PL} \le SoC_t^{PL} \le \overline{SoC}_t^{PL} : \langle \underline{\mu}_t^{SoC}, \overline{\mu}_t^{SoC}\rangle \tag{17d}$$

$$0 \le p_t^{PL,c} \le \overline{p}_t^{PL} : \langle \underline{\mu}_t^{PL,c}, \overline{\mu}_t^{PL,c}\rangle\,;\ \forall t \in \mathcal{T} \tag{17e}$$

$$0 \leq p_t^{PL,d} \leq \overline{p}_t^{PL} : \langle \underline{\mu}_t^{PL,d}, \overline{\mu}_t^{PL,d} \rangle ; \forall t \in \mathcal{T} \quad (17f)$$

$$0 \leq p_t^{PL,im} \leq \overline{p}_t^{PL} : \langle \underline{\mu}_t^{PL,im}, \overline{\mu}_t^{PL,im} \rangle ; \forall t \in \mathcal{T} \quad (17g)$$

$$0 \leq p_t^{PL,ex} \leq \overline{p}_t^{PL} : \langle \underline{\mu}_t^{PL,ex}, \overline{\mu}_t^{PL,ex} \rangle ; \forall t \in \mathcal{T} \quad (17h)$$

where dual variables are given between brackets $\langle \cdot \rangle$.

Above, the PL cost (17a) is minimized, encompassing three terms. The first term accounts for the cost of charging/discharging in the CS under dynamic charging prices. As seen, EVs pay for charging and are paid for discharging, effectively operating as fully functional storage systems, thus enabling energy arbitrage. In this way, the EVs in our model have wide capability to respond to charging prices set by the station operator. Likewise, the second term considers that EVs charge/discharge in different stations through the grid under wholesale electricity prices. As customary, the exporting price is taken σ^{ex} times of the importing one [40]. Typically, $\sigma^{ex} \leq 1$ representing power systems with sufficient generation capacity. Finally, the degradation cost is included for coherently taking into account the degradation of batteries due to multiple charging-discharging. On the other hand, (17b) calculates the instantaneous SoC in the PL, (17c) sets the energy stored at the beginning of the time horizon, and (17d)-(17h) bind variables. Note that (17) is linear and continuous as binary commitment variables are not required [41].

3.2 – CS modelling

In contrast, the CS decides on charging prices while exchanging energy with the grid and provides local PV generation, with the objective of reducing its operational cost. Thus, the CS operational model reads as:

$$\min_{\lambda_t, x^{CS}} F^{CS} = \sum_{t \in \mathcal{T}} \left\{ \mathrm{W}_t^{im} \left(p_t^{CS,im} - \sigma^{ex} p_t^{CS,ex} \right) + \lambda_t \left(p_t^{PL,d} - p_t^{PL,c} \right) \right\} \quad (18a)$$

Subject to:

$$p_t^{CS,im} - p_t^{CS,ex} + p_t^{PV} = p_t^{PL,c} - p_t^{PL,d} ; \forall t \in \mathcal{T} \quad (18b)$$

$$\lambda_t \geq 0 ; \forall t \in \mathcal{T} \quad (18c)$$

$$0 \leq p_t^{CS,im} \leq \overline{p}^G ; \forall t \in \mathcal{T} \quad (18d)$$

$$0 \leq p_t^{CS,ex} \leq \overline{p}^G ; \forall t \in \mathcal{T} \quad (18e)$$

$$0 \leq p_t^{PV} \leq \overline{p}_t^{PV} ; \forall t \in \mathcal{T} \quad (18f)$$

The cost function (18a) considers the cost of exchanging energy with the grid under wholesale prices, as well as the cost (minus profit) of providing charging services under dynamic charging prices. On the other hand, (18b) enforces power balance in the system accounting for the power exchanges with the grid, local PV generation and charging/discharging schedules in the lot. (18c) avoids setting negative charging prices, while (18d)-(18f) bind variables. Note that, although charging/discharging actions of the PL are included in (18b), EV power is not considered a decision variable in the CS problem. Therefore, the station does not determine whether the EVs charge at the station or using other infrastructures. This assumption empowers the PL to decide when and where to charge in order to minimize the total charging cost. The model (18) is also linear and continuous since binary commitment variables are not required [41].

3.3 – MPEC

In the proposed Stackelberg game framework described in Section 2.2, the PL plays as the follower and thus (17) constitutes the lower-level problem, while (18) represents the upper-level as the CS plays the role of the leader. Due to the lower-level problem (17) is continuous and linear, it can be replaced by its equivalent 1st-order optimality conditions, which constitute equivalent conditions for optimality of convex optimization models [42]. In this manner, the

original bi-level problem (1) can be transformed into a single-level mathematical problem with equilibrium constraints (MPEC), as follows:

$$\min_{\lambda_t, x^{CS}, x^{PL}, \phi_t^{SoC}, \boldsymbol{\mu}} F^{CS} \tag{19a}$$

Subject to:

(17b), (17c) (19b)

(18b)-(18f) (19c)

$$\frac{\partial \mathfrak{L}}{\partial SoC_t^{PL}} = \phi_t^{SoC} - \phi_{t+1}^{SoC} - \underline{\mu}_t^{SoC} + \overline{\mu}_t^{SoC} = 0; \forall t \in \mathcal{T} \backslash \{T\} \tag{19d}$$

$$\frac{\partial \mathfrak{L}}{\partial SoC_{(t=T)}^{PL}} = \phi_{(t=T)}^{SoC} - \underline{\mu}_{(t=T)}^{SoC} + \overline{\mu}_{(t=T)}^{SoC} = 0 \tag{19e}$$

$$\frac{\partial \mathfrak{L}}{\partial p_t^{PL,c}} = \lambda_t + \sum_{v \in \mathcal{V}_t} \rho_v^B - \phi_t^{SoC} \tilde{\eta}^{B,c} - \underline{\mu}_t^{PL,c} + \overline{\mu}_t^{PL,c} = 0; \forall t \in \mathcal{T} \tag{19f}$$

$$\frac{\partial \mathfrak{L}}{\partial p_t^{PL,d}} = -\lambda_t + \sum_{v \in \mathcal{V}_{(t=T)}} \rho_v^B + \phi_t^{SoC} / \tilde{\eta}^{B,d} - \underline{\mu}_t^{PL,d} + \overline{\mu}_t^{PL,d} = 0; \forall t \in \mathcal{T} \tag{19g}$$

$$\frac{\partial \mathfrak{L}}{\partial p_t^{PL,im}} = \mathrm{W}_t^{im} + \sum_{v \in \mathcal{V}_t} \rho_v^B - \phi_t^{SoC} \tilde{\eta}^{B,c} - \underline{\mu}_t^{PL,im} + \overline{\mu}_t^{PL,im} = 0; \forall t \in \mathcal{T} \tag{19h}$$

$$\frac{\partial \mathfrak{L}}{\partial p_t^{PL,ex}} = -\sigma^{ex} \mathrm{W}_t^{im} + \sum_{v \in \mathcal{V}_t} \rho_v^B + \phi_t^{SoC} / \tilde{\eta}^{B,d} - \underline{\mu}_t^{PL,ex} + \overline{\mu}_t^{PL,ex} = 0; \forall t \in \mathcal{T} \tag{19i}$$

$$0 \leq SoC_t^{PL} + \underline{SoC}_t^{PL} \perp \underline{\mu}_t^{SoC} \geq 0; \forall t \in \mathcal{T} \tag{19j}$$

$$0 \leq \overline{SoC}_t^{PL} - SoC_t^{PL} \perp \overline{\mu}_t^{SoC} \geq 0; \forall t \in \mathcal{T} \tag{19k}$$

$$0 \leq p_t^{PL,c} \perp \underline{\mu}_t^{PL,c} \geq 0; \forall t \in \mathcal{T} \tag{19l}$$

$$0 \leq \overline{p}_t^{PL} - p_t^{PL,c} \perp \overline{\mu}_t^{PL,c} \geq 0; \forall t \in \mathcal{T} \tag{19m}$$

$$0 \leq p_t^{PL,d} \perp \underline{\mu}_t^{PL,d} \geq 0; \forall t \in \mathcal{T} \tag{19n}$$

$$0 \leq \overline{p}_t^{PL} - p_t^{PL,d} \perp \overline{\mu}_t^{PL,d} \geq 0; \forall t \in \mathcal{T} \tag{19o}$$

$$0 \leq p_t^{PL,im} \perp \underline{\mu}_t^{PL,im} \geq 0; \forall t \in \mathcal{T} \tag{19p}$$

$$0 \leq \overline{p}_t^{PL} - p_t^{PL,im} \perp \overline{\mu}_t^{PL,im} \geq 0; \forall t \in \mathcal{T} \tag{19q}$$

$$0 \leq p_t^{PL,ex} \perp \underline{\mu}_t^{PL,ex} \geq 0; \forall t \in \mathcal{T} \tag{19r}$$

$$0 \leq \overline{p}_t^{PL} - p_t^{PL,ex} \perp \overline{\mu}_t^{PL,ex} \geq 0; \forall t \in \mathcal{T} \tag{19s}$$

$$\phi_t^{SoC}: \text{free}; \forall t \in \mathcal{T} \tag{19t}$$

$$\boldsymbol{\mu} \geq 0 \tag{19u}$$

where $\boldsymbol{\mu}$ collects all the μ's and $\perp$ stands for complementarity.

The MPEC (19) shares objective function with the upper-level (18), but the decision-space expands to include the primal and dual variables of the PL. (19b) are the primal feasibility constraints of the lower-level problem (i.e. the equality constraints), while (19c) collects the primal constraints of the upper-level problem thus ensuring their feasibility. On the other hand, (19d)-(19i) are the stationary conditions, which are derived by equalling to zero the Lagrangian function ($\mathfrak{L}$) of (18a); (19j)-(19s) are the complementarity conditions, which are related to the inequality constraints in (17); whereas (19t) and (19u) are the dual feasibility constraints. For a further explanation on how to derive the 1st-order optimality conditions of linear continuous optimization models, the reader is referred to [23].

3.4 – MILP

MPEC (19) is nonlinear due to bilinear terms in (19a) and complementarity conditions (19j)-(19s). To linearize the complementarity conditions, we employ the exact approximation based on the big-M method [43], following the strategies in [44] to tune the value of the big-M's. On the other hand, to linearize the bilinear terms in (19a), we exploit the strong duality theorem [31],

which establishes that the value of the primal and dual objective functions is the same at the optimum. Firstly, (19a) is rewritten as follows:

$$F^{CS} = \sum_{t\in\mathcal{T}}\left\{\mathrm{W}_t^{im}\left(p_t^{CS,im} + p_t^{PL,im}\right) - \mathrm{W}_t^{ex}\left(p_t^{CS,ex} + p_t^{PL,ex}\right) + D_t^{PL}\right\} - F^{PL} \tag{20}$$

While the dual counterpart of (17a) can be derived, as follows:

$$F^{PL} = \sum_{t\in\mathcal{T}}\left\{\begin{array}{c}\underline{\mu}_t^{SoC}\underline{SoC}_t^{PL} - \overline{\mu}_t^{SoC}\overline{SoC}_t^{PL} - \overline{\mu}_t^{PL,c}\overline{p}_t^{PL} - \\ \overline{\mu}_t^{PL,d}\overline{p}_t^{PL} - \overline{\mu}_t^{PL,im}\overline{p}_t^{PL} - \overline{\mu}_t^{PL,ex}\overline{p}_t^{PL}\end{array}\right\} \tag{21}$$

And replacing (21) in (20) gives rise:

$$F^{CS} = \sum_{t\in\mathcal{T}}\left\{\begin{array}{c}\mathrm{W}_t^{im}\left(p_t^{CS,im} + p_t^{PL,im}\right) - \mathrm{W}_t^{ex}\left(p_t^{CS,ex} + p_t^{PL,ex}\right) - \\ \underline{\mu}_t^{SoC}\underline{SoC}_t^{PL} + \overline{\mu}_t^{SoC}\overline{SoC}_t^{PL} + \overline{\mu}_t^{PL,c}\overline{p}_t^{PL} - \\ \overline{\mu}_t^{PL,d}\overline{p}_t^{PL} + \overline{\mu}_t^{PL,im}\overline{p}_t^{PL} + \overline{\mu}_t^{PL,ex}\overline{p}_t^{PL} + D_t^{PL}\end{array}\right\} \tag{22}$$

According to the strong duality theorem, the value of the linear function (22) and (19a) is the same at the optimum and therefore both can be considered indistinguishably. After replacing (19a) by (22) and the complementarity conditions by the big-M constraints, (19) transforms into a mixed-integer-linear programming (MILP), which is solvable using off-the-shelf solvers. The final MILP problem constitutes a Stackelberg game model between the CS and PL whose solution is a Nash equilibrium point, as illustrated in Appendix A.

4 – The proposed robust solution strategy

4.1 – Determining uncertainty bounds via bootstrapping

In the interval uncertainty modelling described in Section 2.3, it is crucial to properly determine the bounds of uncertain parameters. In many references, these bounds are simply estimated using imposed confidence intervals [32]. While this approach may be acceptable in short-time windows, it overlooks specific features of uncertainties specially in long-term horizons. In this paper, we propose a methodology based on bootstrapping, similar to the one suggested in [25].

Bootstrapping is a statistical technique that allows inferring reliable statistical indicators when available observations do not meet normality criteria, or the number of observations is inadequate (either too small to be reliable or too large to be tractable). Bootstrapping is grounded in the central limit theorem, which states that the observations from any experiment tend to follow a normal distribution if the number of samples is sufficiently large [45].

Fig. 3 illustrates the bootstrapping working cycle, taking a set of observations represented as coloured circles. Firstly, a number of bootstrap subsamples are by randomly selecting samples from the original dataset. It is noteworthy that observations in subsamples can be repeated, which is known as sampling with replacement [45]. Secondly, the mean value of each subsample is calculated and aggregated to form a final distribution. If the number of subsamples and their sizes are adequate, the final distribution of means should follow a normal distribution. Consequently, reliable indicators (e.g. percentiles) can be derived from this distribution.

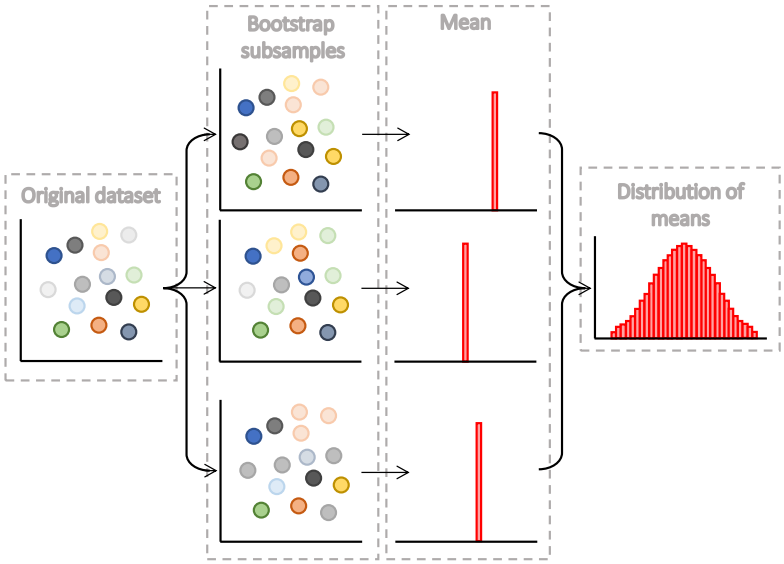

Fig. 3 – Example of application of bootstrapping

Firstly, let N be the number of subsamples and K the number of observations within each subsample. The proposed methodology considers the dataset θ including Θ observations. Note that this dataset could contain historical measurements or synthetic data. The proposed methodology starts calculating the vector w_n, as follows:

$$w_n = \text{randi}(\Theta, K) \tag{23}$$

Indeed, w_n contains the indexes of those observations in θ that will be included in the n^{th} subsample. Let $\theta_k^{w_n}$ be the k^{th} observation of the n^{th} subsample. Then, the mean of the n^{th} subsample can be calculated easily as:

$$\hat{\theta}_n = \frac{1}{K}\sum_{k=1}^{k=K} \theta_k^{w_n} \tag{24}$$

The process (23) and (24) is repeated N times. If N and K are sufficiently large, the distribution of $\hat{\theta}_n$ should follow a normal distribution. In particular, we determine the bounds of an uncertainty using percentiles on the resulting distribution of means. Let us consider that the selected low and high percentiles are $\underline{q}$ and $\overline{q}$, respectively. Then, the bounds on the original dataset can be determined as:

$$\underline{\theta} = \mathbb{Q}_{\underline{q}}[\hat{\theta}], \overline{\theta} = \mathbb{Q}_{\overline{q}}[\hat{\theta}] \tag{25}$$

Note that $\underline{q}$ and $\overline{q}$ are input parameters that can be tuned according to decision-maker own preferences, allowing to expand or reduce the uncertain domain accordingly. Moreover, more conservative strategies could be adopted deriving the maximum and minimum values on subsamples instead of means. Likewise, the expected value can be derived as the mean of the means distribution, as follows:

$$\mathbb{E}[\theta] = \frac{1}{N}\sum_{n=1}^{n=N} \hat{\theta}_n \tag{26}$$

To show the effectiveness of the proposed methodology, it has been applied to wholesale electricity prices in Spain in 2023, which are available in [46]. Fig. 4 (top) shows the distribution for hourly wholesale prices in the original dataset. As observed, the original data do not follow a normal distribution. Furthermore, we applied the proposed bootstrapping strategy considering $N = 50{,}000$ and $K = 60$, and the final distribution of means is plotted in Fig. 4 (bottom). As seen, final distributions clearly meet normality criteria and therefore valid statistical indicators (such as the mean or percentiles) can be derived.

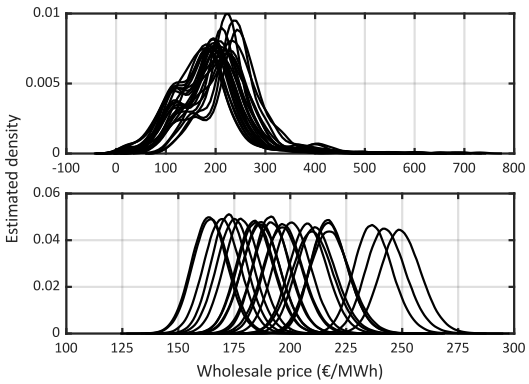

Fig. 4 – Distribution of wholesale electricity prices in Spain in 2023 before (top) and after applying bootstrapping (bottom)

4.2 – Foundations of the proposed solution strategy

In Section 3 we explained how to reduce the bi-level strategic pricing problem into a solvable single-level one. However, the problem described in (1) remains difficult to solve due to the presence of a nested max-min optimization. Typically, these types of frameworks are addressed by replacing the inner minimization problem with its 1st-order optimality conditions [30]. However, our inner problem is a non-continuous and non-convex MILP and, in consequence, its 1st-order optimality conditions are not sufficient conditions for optimality.

To circumvent this issue, we develop a tailored algorithm that retains the hierarchical structure of the Stackelberg game proposed in Section 3. The main idea is to decompose the original max-min problem into two components: the inner problem, which focuses on deriving charging prices, and the maximization problem, which aims to identify the worst-case realization of uncertainties. The sequential logic underlying the developed algorithm is summarized in the following:

- Firstly, the charging prices are revealed assuming deterministic conditions and solving the original MPEC as presented in Section 3.
- Under fixed charging prices, the station determines the worst-case realization of its own uncertainties (i.e. Ω^{CS}), while the PL waits and sees.
- The PL reacts to the worst-case realization of uncertainties by seeking for the best-case realization of its own uncertainties (i.e. Ω^{PL}).
- For a given charging price and worst-case uncertainties, the station finally adjusts its scheduling plan minimizing costs.

As seen, the methodology described above aligns with the proposed Stackelberg game framework. Specifically, the station moves first to determine charging prices and the worst-case realization of uncertainties, while the PL reacts to the CS decisions. It is noteworthy that we assume that the best-case realization of Ω^{PL} corresponds to the worst-case scenario for the station. This assumption is consistent, as reducing the parking costs leads to maximizing the CS cost (see (20)). For simplicity, Fig. 5 shows a flowchart of the proposed solution strategy. The developed algorithm is validated in Appendix B through an illustrative example.

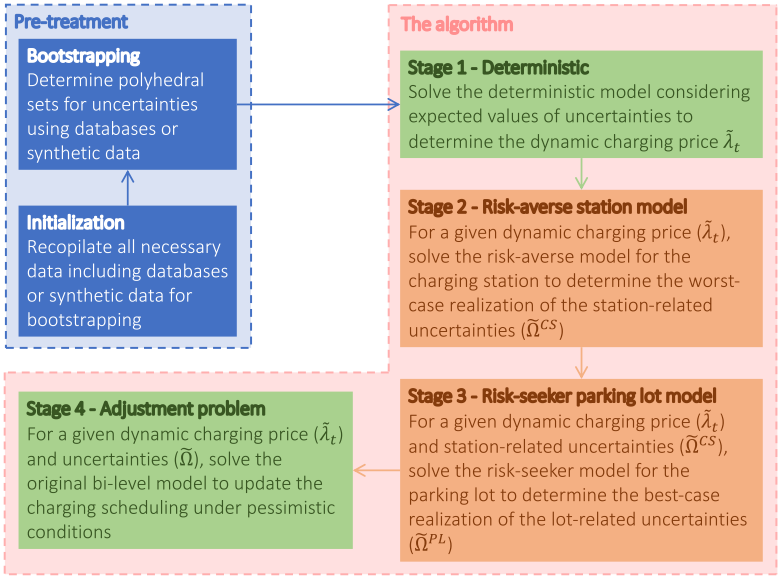

Fig. 5 – Flowchart of the proposed solution methodology

4.3 – Formulation of the proposed solution strategy

Subsequent sections detail the mathematical formulation of the stages involved in the developed solution algorithm described in Fig. 5.

4.3.1 – Stage 1

Stage 1 determines dynamic charging prices assuming deterministic conditions by solving the strategic pricing MPEC problem, as follows:

$$\tilde{\lambda}_t, \tilde{x}^{CS}, \tilde{x}^{PL} \in \arg \min_{\substack{\lambda_t, x^{CS}, x^{PL}, \\ \phi_t^{SoC}, \boldsymbol{\mu}}} F^{CS}(\mathbb{E}[\Omega]) \tag{27a}$$

Subject to:

(19b), (19c) (27b)
(19d)-(19i) (27c)
(19j)-(19s) (27d)
(19t), (19u) (27e)

Problem (27) comprises the original station cost function (27a), the primal feasibility constraints (27b), the stationary and complementarity conditions (27c) and (27d), and the dual feasibility conditions (27e). After solving (27), one obtains the charging prices (i.e. $\tilde{\lambda}_t$), and primal solutions for the CS and PL (i.e. $\tilde{x}^{CS}$ and $\tilde{x}^{PL}$, respectively).

4.3.2 – Stage 2

Stage 2 solves the CS problem solely, under given charging prices and x^{PL}, looking for the worst-case realization of Ω^{CS}, as follows:

$$\tilde{\Omega}^{CS} \in \arg \max_{x^{CS}, \Omega^{CS}} F^{CS}\left(\tilde{\lambda}_t, \tilde{x}^{PL}\right) \tag{28a}$$

Subject to:

(19c) (28b)
$\omega \in [\underline{\omega}, \overline{\omega}]; \forall \omega \in \Omega^{CS}$ (28c)
$\mathbb{E}[\omega] - \alpha \Delta_{\omega}^{\downarrow} \leq \omega \leq \mathbb{E}[\omega] + \alpha \Delta_{\omega}^{\uparrow}; \forall \omega \in \Omega^{CS}$ (28d)

Problem (28) maximizes the cost function of the CS and comprises its primal constraints (28b) and interval uncertainty modelling (28c) and (28d). Note that (28) naturally derives worst-case realization of Ω^{CS} as the cost function is maximized. Note that solution of (28) is feasible for the PL as the value of x^{PL} is fixed. (28) is nonlinear due to the bilinear product of wholesale prices and powers in (28a). Due to both powers and prices are box-constrained, their bilinear product can be linearized using McCormick envelopes [47]. Let y and z be continuous variables, their product can be replaced by the dummy variable u and the following constraints:

$$u \geq \underline{y}z + y\underline{z} - \underline{y}\underline{z} \tag{29a}$$
$$u \geq \overline{y}z + y\overline{z} - \overline{y}\overline{z} \tag{29b}$$
$$u \leq \underline{y}z + y\overline{z} - \underline{y}\overline{z} \tag{29c}$$
$$u \leq \overline{y}z + y\underline{z} - \overline{y}\underline{z} \tag{29d}$$
$$\underline{y} \leq y \leq \overline{y}, \underline{z} \leq z \leq \overline{z} \tag{29e}$$

4.3.3 – Stage 3

Similar to Stage 2, Stage 3 solves the PL problem solely assuming given values of λ_t, x^{CS} and Ω^{CS}, to determine the best-case realization of Ω^{PL}, as follows:

$$\widetilde{\Omega}^{PL} \in \arg\min_{x^{PL},\Omega^{PL}} F^{PL}\left(\tilde{\lambda}_t, \tilde{x}^{CS}, \widetilde{\Omega}^{CS}\right) \tag{30a}$$

Subject to:

$$\text{(15b)-(15h)} \tag{30b}$$
$$\omega \in \left[\underline{\omega}, \overline{\omega}\right]; \forall \omega \in \Omega^{PL} \tag{30c}$$
$$\mathbb{E}[\omega] - \alpha\Delta_{\omega}^{\downarrow} \leq \omega \leq \mathbb{E}[\omega] + \alpha\Delta_{\omega}^{\uparrow}; \forall \omega \in \Omega^{PL} \tag{30d}$$

Problem (30) minimizes the cost function of the PL and comprises its primal constraints (30b) and interval uncertainty modelling (30c) and (30d). Note that (30) naturally derives worst-case realization of Ω^{PL} as the cost function is minimized. Note that solution of (30) is feasible for the CS as the value of x^{CS} is fixed.

4.3.4 – Stage 4

For given charging prices and worst-case uncertainties, Stage 4 adjusts the scheduling plan for the CS, as follows:

$$\min_{x^{CS},x^{PL}} F^{CS}\left(\tilde{\lambda}_t, \widetilde{\Omega}^{CS}, \widetilde{\Omega}^{PL}\right) \tag{31a}$$

Subject to:

$$\text{(17b)-(17h)} \tag{31b}$$
$$\text{(19c)} \tag{31c}$$

Problem (31) minimizes the station cost constrained by primal models of the PL (31b) and CS (31c).

4.4 – Practical considerations

In the following, several practical considerations to take into account when implementing the developed solution strategy are discussed.

- The developed model devotes to determine dynamic charging prices, which will remain fixed for a significant period of time (e.g. one year). Therefore, the focus of the model is not on controlling charging demand, but rather on implementing a dynamic pricing strategy. In this sense, the implementation of the developed strategy does not require establishing complex communication channels with the charging points.

- Political or social barriers may arise, particularly when enabling vehicle-to-grid technologies. Despite that the developed model accounts for battery degradation avoiding their over-utilization, EV owners may be hesitant to accept partial discharge of on-board batteries. Furthermore, vehicle-to-grid is not yet legally permitted in some countries [48]. Nonetheless, the developed model can still be implemented with only charging mode enabled without any problem.
- The implementation of the developed model requires knowledge of the uncertain parameters involved. In the absence of historical databases, fitted probability distributions or synthetic data should be used. Nevertheless, different non-data approaches exist to model typical uncertainties such as PV generation [49] or EV behavior [50], which can be used and allow employing even if historical data is not available.

5 – Case study

This section presents a case study with results. The optimization models developed in this paper were coded under Matlab R2021b and solved using Gurobi [51].

5.1 – Input data

We consider a charging station equipped with 55-kW fast chargers as the most conventional option for public charging infrastructures. The capacity of the station was in the range of 500 vehicles, expecting a number of charging events between 250 and 500 per day. This way, we consider a large-scale station with capacity to decide dynamic charging prices, scenario more difficulty implementable in small-scale infrastructures. SoC bounds have been generated using the methodology in [50] for an expected number of vehicles ranging from 250 to 500. For other uncertainties, we have used real databases. In particular, PV potential corresponds with real data in Madrid (Spain) in 2023 [52], with optimal azimuth and tilt angle. Furthermore, wholesale prices have been considered as in the example in Section 4.2, corresponding to wholesale electricity prices in Spain in 2023 from [46]. Using the same parameters reported in Section 4.2, the proposed bootstrapping methodology was applied to derive uncertainty bounds, which are shown in Fig. 6. For illustrative purposes, the bounds were derived as the 2.5th and 97.5th percentiles on minimum and maximum values of the original datasets. Thereby, only 2.5 % of possible uncertainty realizations will lie out of the considered uncertainty set. This is considered a reasonable setting for most of decision-making tools with risk consideration, stablishing sufficiently conservative assumptions without lying in over-robustness.

For the unitary degradation cost (i.e. ρ_v^B), we performed a statistical analysis considering typical EV commercial features from [53]. After sampling a large number of observations, the bootstrapping methodology in Section 4.2 was applied to the degradation cost, resulting in an expected value of 2.73 €/MWh, aligning with other degradation costs reported in the literature [54]. We assume an electricity market with generation surplus, as typical in many power systems. Under such conditions, additional taxes, fees and charges are imposed on purchasing rates when exporting energy to the grid. Keeping this in mind and in line with other references [40], $\sigma^{ex} = 0.7$ was assumed in this paper. On the other hand, most of commercial EVs install Li-ion batteries [53]. According to [36], charging and discharging efficiency of batteries was set at 95 %. Finally, $\overline{p}^G = 15$ MW was considered.

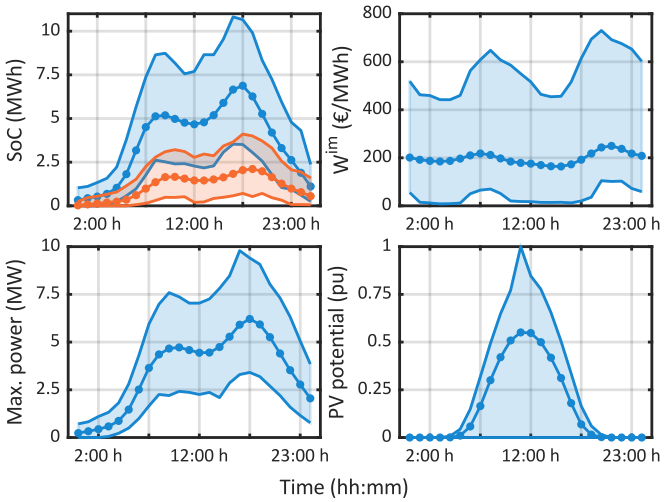

Fig. 6 – Uncertainty intervals considered in simulations

5.2 – Economic analysis

Fig. 7 plots the estimated station daily profit for different risk levels and PV sizes. As expected, increasing the risk level leads to a reduction in the estimated profit. Furthermore, the effect of increasing the risk level becomes more pronounced as more PV capacity is installed. These results are coherent with the idea of robust optimization and validate the proposed solution strategy. Indeed, increasing the risk level should negatively affect the station profit, as uncertainties can fluctuate across a wider range, and therefore, worse solutions are accessible. On the other hand, as the PV size increases, its volatility has a greater effect on final results. Fig. 7 also confirms that PV has a positive impact on the economy of the station, showing a near-linear profit increment with the PV size.

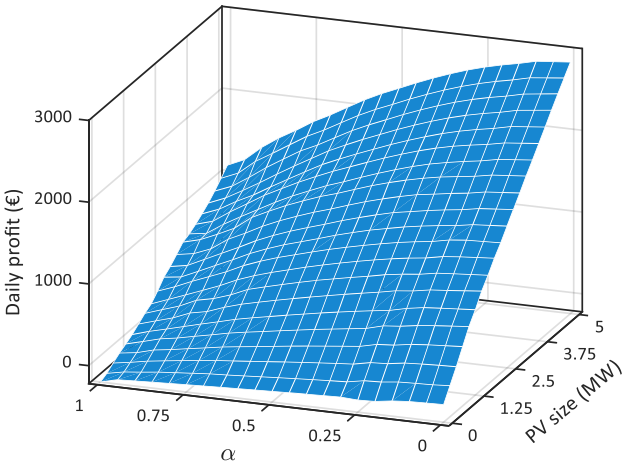

Fig. 7 – Estimated daily CS profit for different risk levels and PV sizes

Fig. 8 is analogous to Fig. 7, but referred to the PL cost. As expected, results in this figure show the opposite behaviour compared to those in Fig. 7. This demonstrates that both the PL and CS pursue different objectives, and therefore, equilibrium analysis is relevant for the problem at hand, strengthening the use of game-theoretical approaches in the present context. It is noteworthy that the PL might access to high profits, emphasizing the importance of enabling dynamic charging prices to attract EVs to public CSs. Note that, for illustrative purposes, we intentionally do not include non-negativity limitation in the PL cost, but this kind of restrictions could be imposed in real scenarios to prevent EV strategic participation, potentially leading to station losses. On the other hand, it is important to note that PV size still has a positive impact on the PL economy, though this effect is less significant compared to the CS.

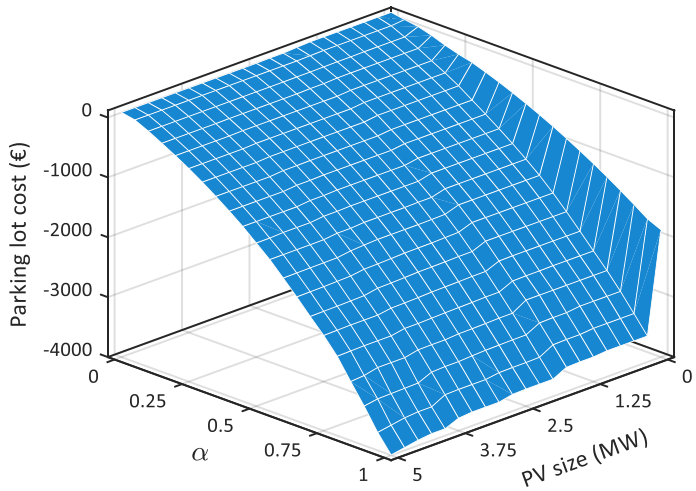

Fig. 8 – Estimated daily PL cost for different risk levels and PV sizes

Beyond the influence of the PV size and uncertainty budget, the impact of the wholesale electricity price has also been examined. For this purpose, the benchmark profiles from [46] were multiplied by a real parameter, δ. The results of this analysis are presented in Fig. 9, comparing the CS profit and PL cost for different values of δ. To inhibit the impact of other parameters the PV size and uncertainty budget were taken 5 MW and 1, respectively. Surprisingly, increasing the wholesale price has a positive effect on the CS profit. This is because low wholesale prices force to reduce the charging price to attract vehicles to the station, as further discussed later on. Conversely, increasing the wholesale price leads to a reduction of the PL cost up to approximately $\delta = 0.9$. Beyond this point, the PL cost remains stable, while the CS profit increments more notably with higher electricity prices. This is due to the fact that higher prices incentivize further discharging as vehicles generate higher income. However, the increase in the monetary profit is somewhat mitigated by substantial charging costs beyond $\delta = 0.9$. These results highlight the importance of considering vehicle-to-grid as a potential alternative revenue stream for EV owners, which may encourage them to use public fast chargers instead of domestic ones.

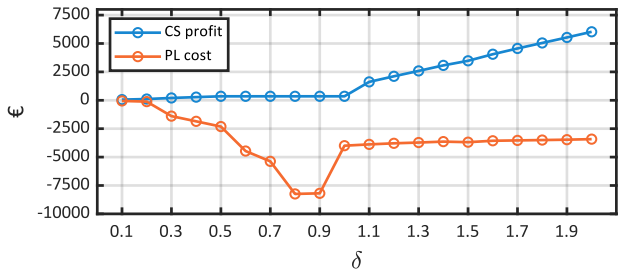

Fig. 9 – Total CS profit and PL cost for different wholesale electricity prices

Furthermore, results in Fig. 9 demonstrates the ability of the proposed methodology to reach a Nash equilibrium solution between the CS and PL. Indeed, below $\delta = 0.9$, the PL cost is reduced while the CS profit is maintained stable. Above $\delta = 0.9$, the contrary occurs and the CS increments its profit while the PL cost is maintained stable. It reveals that any agent in the game seeks to increase its own profit by causing losses for other agents. Actually, it can be seen in Fig. 9 that a profit is ensured for both agents under different wholesale prices.

5.3 – Uncertainty analysis

To further validate the developed robust solution approach, Fig. 10 plots the worst-case realization of uncertainties for different risk levels and PV sizes. Concerning the parking-related

uncertainties, it is evident that they evolve toward their best-case realization, which represents the worst scenario for the station, as discussed in Section 4.3. Indeed, as the risk level increases, SoC limits are relaxed and more power becomes available in the parking, thus enabling a very flexible response of the PL. In these circumstances, the parking has greater capacity to respond to charging prices and get advantages of them.

Regarding station-related uncertainties, both wholesale prices and PV generation increase with the risk level. Specifically, the cost of importing energy rises proportionally with the wholesale price. However, an increase in the wholesale pricing also implies a rise in the export price. Nevertheless, costs from imports are notably higher than incomes from export in charging activities. Thus, an increase in the wholesale price has a more negative impact on the station profit than a decrease in prices. On the other hand, increasing PV generation forces to reduce charging prices, as discussed later on. In the event of low charging prices, the CS receives reduced payments from charging, which negatively affects its economy. It is noteworthy that the impact of the PV size on uncertainties is marginal (with the obvious exception of the total PV generation), which indicates that α affects uncertainties solely. This conclusion is particularly relevant as it demonstrates that the developed solution strategy is case-independent and capable of accessing worst-case scenarios, regardless the size of the PV facility.

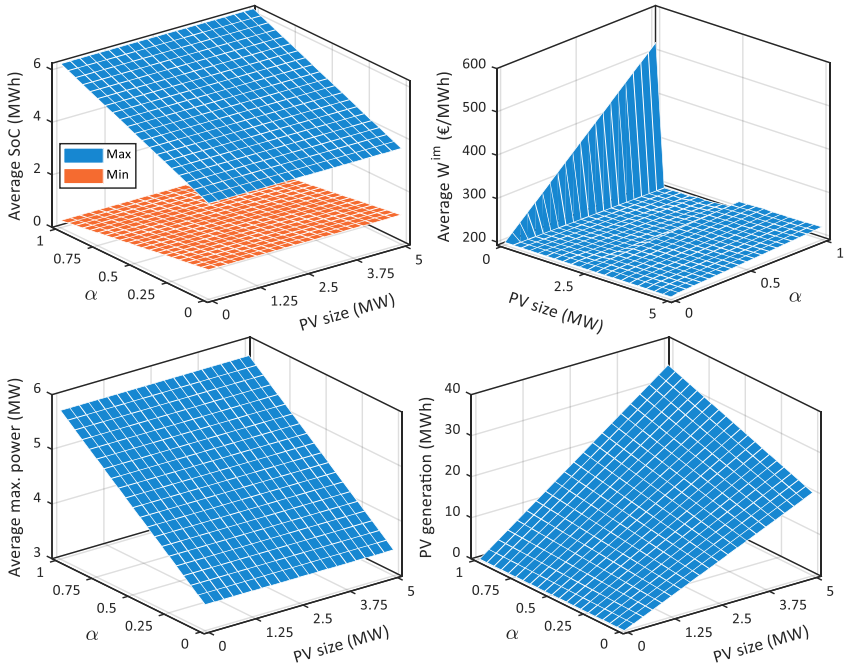

Fig. 10 – Worst-case realization of uncertainties for different risk levels and PV sizes

5.4 – Pricing strategy

Let us focus now on the resulting charging pricing strategy. Firstly, we examine the effect of the risk level solely. To this end, Fig. 11 plots resulting prices assuming a 5 MW PV facility and two extreme risk levels. In the deterministic case (i.e. $\alpha = 0$), charging prices are typically set lower than the wholesale prices, which encourages vehicles to charge in the station during the morning and afternoon. At night, charging prices nearly match the wholesale exporting prices (i.e. $\sigma^{ex} \mathrm{W}_t^{im}$). In the face of this situation, vehicles opt to discharge in the station, except at 20:00 h, when the wholesale exporting price is higher that the charging price, causing vehicles to discharge directly to the grid.

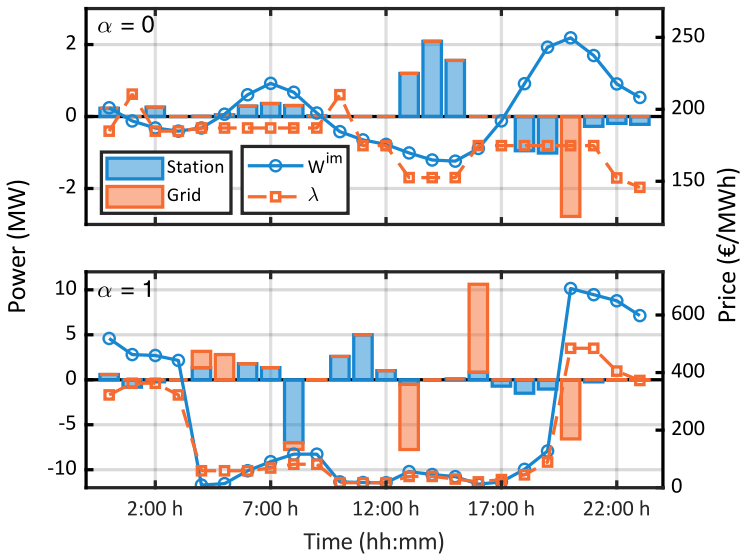

Fig. 11 – Pricing strategy and charging scheduling for different risk levels and 5 MW PV array. In this figure, negative powers imply discharging

Remarkably, wholesale electricity prices are much higher at night and in the evening in the risk-averse case (i.e. $\alpha = 1$), which is reflected in the high average prices shown in Fig. 10. However, electricity prices drop during the morning and afternoon. In response to this situation, the station is compelled to reduce charging prices in order to attract vehicles and encourage them to charge in the station. However, low wholesale prices make it challenging to compete with other options on the grid, resulting in a significant portion of the total charging/discharging demand not being met by the station. Therefore, it is clear to conclude that reducing wholesale prices during morning and afternoon has a significant negative impact on the economy of the station. Indeed, EVs charge mostly and morning and afternoon and low wholesale prices force to reduce charging prices to almost zero to enable competition, thus limiting the accessible profit dramatically.

In Fig. 12 we analyse the effect of increasing PV size on pricing strategy. To this end, results in Fig. 11 are presented for $\alpha = 0$ in order to nullify the effect of robust programming and focus on the PV size solely. As concluded from Fig. 10, PV affects to wholesale prices marginally, but to the charging price. Actually, charging prices could be eventually reduced at afternoon, when PV potential is high. This encourages EVs to charge mostly at these hours. This effect vanishes when PV is not available, displacing a portion of the charging demand to night, when both the wholesale and charging prices are still low.

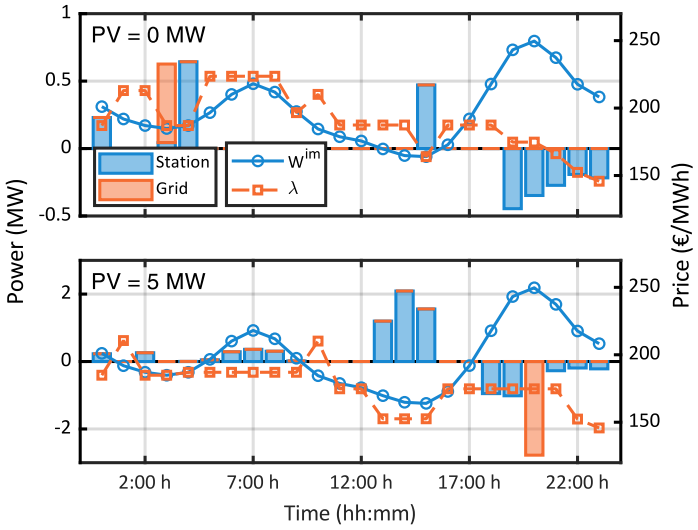

Fig. 12 – Pricing strategy and charging scheduling for different PV sizes and deterministic conditions. In this figure, negative powers imply discharging

5.5 – Computational burden

Finally, we assess the computational performance of the developed algorithm. To this end, a number of simulations were run on an Intel Core i7-10700K CPU 3.80GHz 3.79 GHz with 32 GB RAM, reporting the total computational time in Fig. 13. As seen, the total execution time remains highly competitive This is because the developed methodology involves linear programming problems in stages 2-4, whose computational load rises linearly with the number of decision variables. Therefore, we can hypothesize that the developed solution strategy scales well with the size of the system, showing more than acceptable simulation runtimes even for online applications. Remarkably, computational burden appears to be independent of the risk level and PV size, which facilitates the implementation of the new proposal.

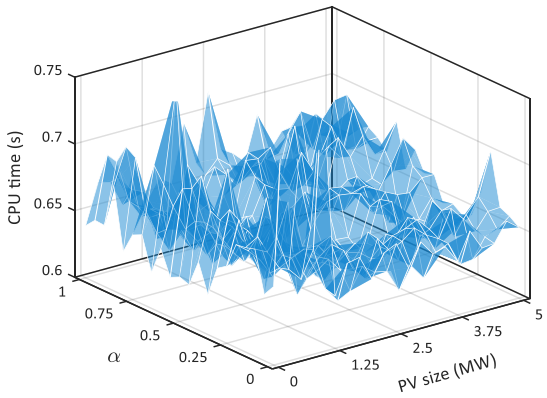

Fig. 13 – Total computational time for different risk levels and PV sizes

To analyse the scalability of the developed methodology, different simulations were run over different time horizons, expanding from 24 hours in advance (day-ahead) until 8760 hours in advance (year-ahead). This way, the size of the problem (i.e. number of variables involved) is varied. Fig. 14 shows the computational time for different time horizons. As observed, the runtime increases exponentially with the problem size, which is coherent since MILP optimization models can be solved in an exponential time using efficient branch-and-bound algorithms [55]. Remarkably, the proposed model was solved within reasonable times even for very long-time horizons (~1000 seconds for one-year horizon), demonstrating that the developed tool is affordable and implementable even on average machines.

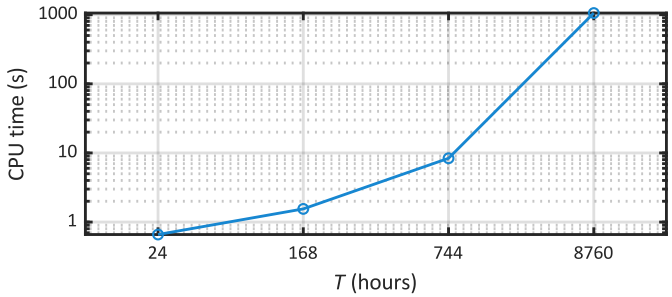

Fig. 14 – Total computational time for different problem sizes

6 – Conclusion

A novel adaptive robust charging price-setting methodology for CSs has been proposed in this paper. The new proposal renders as a game-theoretical max-min bi-level optimization problem, in which the CS plays as the leader, setting charging prices, whereas the PL responds by deciding when, where and how much energy to charge. The developed formulation considers wide response capability of vehicles, enabling charging and discharging through vehicle-to-grid technologies. Different uncertain parameters have been modelled employing interval formulation. A novel data-driven approach based on bootstrapping has been developed to determine the bounds on the uncertainty set. Finally, multi-stage robust solution strategy has been proposed, in order to address the complexity of the original formulation efficiently.

The developed solution approach has been applied to a benchmark large-scale CS. Firstly, different uncertainties have been modelled via intervals, employing the proposed bootstrap-based approach, thus showing its utility. Secondly, an economic analysis has been conducted, validating the robust methodology and assessing the effect of PV size and risk level. Other analyses have been carried out regarding how the different uncertainties impact on outcomes, as well as analysing in-depth the pricing strategy. It has been shown that low wholesale prices negatively affect the CS pricing strategy, forcing it to reduce prices in order to attract vehicles. Finally, the computational burden of the developed model has been assessed, exhibiting a high degree of efficiency and scalability.

This work may suppose a benchmark methodology for robust optimization in bi-level problems. It has been explained that applying robust programming to Stackelberg games may lead to complex formulations difficult to solve using off-the-shelf solvers. In this sense, the development of tailored algorithms and solution strategies should be further explored in the future. Furthermore, the developed algorithm might find applications in different energy problems like strategic participation in energy markets.

CRediT authorship contribution statement

Marcos Tostado-Véliz: Conceptualization, Methodology, Software, Investigation, Writing – Original Draft, Writing - Review & Editing, Visualization, Funding acquisition. **Hany M. Hasanien**: Data curation, Methodology, Validation, Formal analysis, Writing - Original Draft, Writing - Review & Editing, Supervision. **Paul Arévalo**: Investigation, Resources, Data curation, Writing - Original Draft. **Francisco Jurado**: Conceptualization, Formal analysis, Supervision, Project administration, Funding acquisition.

Acknowledgements

Marcos Tostado-Véliz and Francisco Jurado acknowledge to the Spanish Ministry of Science and Innovation, under the research Project “Development of power-flow models for microgrid clusters” PID2021-123633OB-C31, Ministry of Science and Innovation, Knowledge Generation Projects 2021, Spain.

Paul Arévalo thanks to Universidad de Cuenca, Ecuador, for providing access to the facilities of the Micro-Grid Laboratory, Faculty of Engineering.

Appendix A. Stackelberg and Nash equilibria

The bi-level model (1) describes a Stackelberg game between the CS and PL of the form:

$$\mathfrak{G} = \begin{Bmatrix} \{\text{CS} \cup \text{PL}\} \\ \{\lambda\}; \{p^{PL,c}, p^{PL,d}, p^{PL,im}, p^{PL,ex}\} \\ \{F^{CS}, F^{PL}\} \end{Bmatrix} \tag{A1}$$

where the dependence of time has been omitted for simplicity. As seen, $\mathfrak{G}$ describes a game with the CS and PL as players. The CS decides on charging prices, which constitute its strategy, while the strategy of the PL includes charging/discharging powers.

To prove that the bi-level model (1) establishes a Stackelberg game, it is necessary that the objective functions of the leader (CS) and the follower (PL) are continuous non-empty functions of all game strategies [56]. This condition is easy to prove since both F^{CS} and F^{PL} are linear and therefore continuous and non-empty. The third condition is automatically checked since F^{PL} is linear and therefore convex of its own strategy. On the other hand, due to the objectives in (1) are linear, their second partial derivatives with respect to their own strategies are zero and therefore there is a unique solution for the game $\mathfrak{G}$ [56].

To illustrate how the equilibrium works, let us study a toy example based on the formulation of (19). We consider that the PL has a SoC of 2 MWh at time $t-1$, while the maximum/minimum SoC at time t must be 3 MWh. The wholesale electricity price at time t is 50 € MWh and the rest of the data is like the case study in Section 5. For interpreting the results easily, we neglect degradation and battery efficiency as well as enforce to charging in the CS. This toy example can be formulated as a MPEC, as follows:

$$\min_{\substack{\lambda_t, p_t^{CS,im}, p_t^{PL,c}, SoC_t^{PL}, \\ \phi_t^{SoC}, \underline{\mu}_t^{SoC}, \overline{\mu}_t^{SoC}, \underline{\mu}_t^{PL,c}, \overline{\mu}_t^{PL,c}, \underline{\mu}_t^{PL,d}, \overline{\mu}_t^{PL,d}}} F^{CS} = \begin{Bmatrix} \mathrm{W}_t^{im} p_t^{CS,im} + \phi_t^{SoC} SoC_{t-1}^{PL} - \underline{\mu}_t^{SoC} \underline{SoC}_t^{PL} + \\ \overline{\mu}_t^{SoC} \overline{SoC}_t^{PL} + \overline{\mu}_t^{PL,c} \overline{p}_t^{PL} + D_t^{PL} \end{Bmatrix} \tag{A2}$$

Subject to:

$$p_t^{CS,im} = p_t^{PL,c} \tag{A3}$$
$$SoC_t^{PL} = SoC_{t-1}^{PL} + p_t^{PL,c} : \langle \phi_t^{SoC} \rangle \tag{A4}$$
$$\frac{\partial \mathfrak{L}}{\partial SoC_t^{PL}} = \phi_t^{SoC} - \underline{\mu}_t^{SoC} + \overline{\mu}_t^{SoC} = 0 \tag{A5}$$
$$\frac{\partial \mathfrak{L}}{\partial p_t^{PL,c}} = \lambda_t + -\phi_t^{SoC} - \underline{\mu}_t^{PL,c} + \overline{\mu}_t^{PL,c} = 0 \tag{A6}$$
$$\frac{\partial \mathfrak{L}}{\partial p_t^{PL,d}} = -\lambda_t + \phi_t^{SoC} - \underline{\mu}_t^{PL,d} + \overline{\mu}_t^{PL,d} = 0 \tag{A7}$$
$$0 \le SoC_t^{PL} + \underline{SoC}_t^{PL} \perp \underline{\mu}_t^{SoC} \ge 0 \tag{A8}$$
$$0 \le \overline{SoC}_t^{PL} - SoC_t^{PL} \perp \overline{\mu}_t^{SoC} \ge 0 \tag{A9}$$
$$0 \le p_t^{PL,c} \perp \underline{\mu}_t^{PL,c} \ge 0 \tag{A10}$$
$$0 \le \overline{p}_t^{PL} - p_t^{PL,c} \perp \overline{\mu}_t^{PL,c} \ge 0 \tag{A11}$$
$$0 \le p_t^{PL,d} \perp \underline{\mu}_t^{PL,d} \ge 0 \tag{A12}$$
$$0 \le \overline{p}_t^{PL} - p_t^{PL,d} \perp \overline{\mu}_t^{PL,d} \ge 0 \tag{A13}$$
$$\phi_t^{SoC} : \text{free} \tag{A14}$$
$$\underline{\mu}_t^{SoC}, \overline{\mu}_t^{SoC}, \underline{\mu}_t^{PL,c}, \overline{\mu}_t^{PL,c}, \underline{\mu}_t^{PL,d}, \overline{\mu}_t^{PL,d} \ge 0 \tag{A15}$$

where (A2) is the corresponding linearized objective function, which can be derived following the premises in Section 3.4, while the rest of constraints are as in the MPEC model (19). Note that the primal solution of this model is trivial with $p_t^{PL,c} = 1$ MW to satisfy the limits on SoC and

this is because exporting powers were neglected above. After running the model (A2)-(A15), the solution is $\lambda_t = 50$ €/MWh, with an objective value of $F^{CS} = 0$ €. This illustrates that the proposed MPEC model effectively achieves an equilibrium between the PL and the CS, as the CS fixes the charging price equal to the wholesale one in order to minimize the cost of the parking lot instead of maximizing its own profit unilaterally.

Appendix B. Illustration of the developed solution algorithm

This appendix presents an illustrative example to validate the developed solution algorithm. The developed iterative solution strategy performs effectively in optimization problems with objective functions that involve two conflicting objectives. These types of problems have the following form:

$$\max_{x,y,z} f_1(x,y,z) - f_2(y) \tag{B1}$$

Subject to:

$$g(x,y,z) \leq 0 \tag{B2}$$
$$h(x,y,z) = 0 \tag{B3}$$

As seen, maximizing f_2 results in the minimization of the objective (B1), whereas the opposite occurs when maximizing f_1. The developed algorithm tailors this kind of problems, which align with the model studied in this paper, where maximizing the CS profit implies maximizing the PL cost, and vice versa. Below, a simple problem is illustrated just to show how the developed solution strategy works.

$$\max_{x,y,z} \underbrace{(5z - x + y)}_{f_1} - \underbrace{(y - 3)}_{f_2} \tag{B4}$$

Subject to:

$$0 \leq x \leq 5 \tag{B5}$$
$$1 \leq y \leq 6 \tag{B6}$$
$$0 \leq z \leq 1 \tag{B7}$$

The solution of (B4)-(B7) is trivial: $x = 0$, $y = 6$ and $z = 1$ with $f_1 = 11$ and $f_2 = -3$. As observed, the problem above shares structure with (B1)-(B3), so the developed algorithm can be employed to solve it. To this end, x and y are considered variables, being 3 the expected value of y. The first step maximizes (B4) taking the expected value of y, thus obtaining $z = 1$ and $x = 0$. In the second stage, (B4) is minimized taking the value of x and z obtained in the first stage. The solution in this case is $y = 6$ with $f_1 = 11$ and $f_2 = -3$, and thus the correct solution has been attained. While the example above can be solved directly due to its simplicity, the developed algorithm proves to be valuable in more challenging problems as such addressed in this paper.

References

[1] IEA. Global EV Outlook 2024. IEA, Paris, 2024. Online, available at: https://www.iea.org/reports/global-ev-outlook-2024, (accessed 7 Feb. 2025).

[2] J. Altamirano. Charging infrastructure is growing in Europe but not at the desired pace: What are the consequences? Published in Mobility Portal Europe, 16 Jul. 2024. Online, available at: https://mobilityportal.eu/charging-infrastructure-growing-europe/, (accessed 7 Feb. 2025).

[3] Instituto para la Diversificación y Ahorro de Energía (IDAE). Programa Moves III. Online, available at: https://www.idae.es/en/support-and-funding/mobility-and-vehicles/programa-moves-iii, (accessed 7 Feb. 2025).

[4] J. Altamirano. Incentives and Tax Benefits: How Are EU Countries Promoting Electromobility? Published in Mobility Portal Europe, 7 Aug. 2024. Online, available at: https://mobilityportal.eu/incentives-tax-benefits-electromobility/, (accessed 7 Feb. 2025).

[5] K.D. Afentoulis, Z.N. Bampos, S.I. Vagropoulos, S.D. Keranidis, P.N. Biskas. Smart charging business model framework for electric vehicle aggregators. *Applied Energy* 2022; 328: 120179. 10.1016/j.apenergy.2022.120179.

[6] Is It Cheaper to Charge an EV at Home or in Public? Published in Qmerit, 27 Oct. 2023, updated 18 Nov. 2024. Online, available at: https://qmerit.com/blog/comparing-long-term-cost-analysis-of-ev-home-charging-vs-public-charging/, (accessed 7 Feb. 2025).

[7] Z. Lu, J. Qi, J. Zhang, L. He, H. Zhao. Modelling dynamic demand response for plug-in hybrid electric vehicles based on real-time charging pricing. *IET Generation, Transmission & Distribution* 2017; 11(1): 228-35. 10.1049/iet-gtd.2016.0882.

[8] X. Dong et al. A charging pricing strategy of electric vehicle fast charging stations for the voltage control of electricity distribution networks. *Applied Energy* 2018; 225: 857-68. 10.1016/j.apenergy.2018.05.042.

[9] S. Zhou et al. Dynamic EV Charging Pricing Methodology for Facilitating Renewable Energy With Consideration of Highway Traffic Flow. *IEEE Access* 2020; 8: 13161-78. 10.1109/ACCESS.2019.2958403.

[10] J. Lin, B. Xiao, H. Zhang, X. Yang, P. Zhao. A novel underfill-SOC based charging pricing for electric vehicles in smart grid. *Sustainable Energy, Grids and Networks* 2021; 28: 100533. 10.1016/j.segan.2021.100533.

[11] R. Feng, D. Czarkowski. Regularised dynamic optimal transportation of electric vehicles over networks considering strategic charging pricing. *IET Energy Systems Integration* 2021; 3(1): 73-85. 10.1049/esi2.12005.

[12] Q. Zhang, T. Sun, Z. Ding, C. Li. Nodal dynamic charging price formulation for electric vehicle through the Stackelberg game considering grid congestion. *IET Smart Grid* 2021; 4(5): 461-73. 10.1049/stg2.12025.

[13] Y. Sheng, Q. Guo, F. Chen, L. Xu, Y. Zhang. Coordinated pricing of coupled urban Power-Traffic Networks: The value of information sharing. *Applied Energy* 2021; 301: 117428. 10.1016/j.apenergy.2021.117428.

[14] J. Vuelvas, F. Ruiz, G. Gruosso. A time-of-use pricing strategy for managing electric vehicle clusters. *Sustainable Energy, Grids and Networks* 2021; 25: 100411. 10.1016/j.segan.2020.100411.

[15] Y. Lu, Y. Liang, Z. Ding, Q. Wu, T. Ding, W.-J. Lee. Deep Reinforcement Learning-Based Charging Pricing for Autonomous Mobility-on-Demand System. *IEEE Transactions on Smart Grid* 2022; 13(2): 1412-26. 10.1109/TSG.2021.3131804.

[16] C. Wang, S. Ma, Z. Cai, N. Yan, Q. Wang. Bounded rational real-time charging pricing strategy under the traffic-grid coupling network. *IET Electrical Systems in Transportation* 2022; 12(4): 251-68. 10.1049/els2.12050.

[17] J. Liu, G. Lin, S. Huang, Y. Zhou, C. Rehtanz, Y. Li. Collaborative EV Routing and Charging Scheduling With Power Distribution and Traffic Networks Interaction. *IEEE Transactions on Power Systems* 2022; 37(5): 3923-36. 10.1109/TPWRS.2022.3142256.

[18] C. Lu, J. Wu, J. Cui, Y. Xu, C. Wu, M.C. Gonzalez. Deadline Differentiated Dynamic EV Charging Price Menu Design. *IEEE Transactions on Smart Grid* 2023; 14(1): 502-16. 10.1109/TSG.2022.3193898.

[19] B. Li, J. Li, M. Han. Deep Reinforcement Learning-Based Charging Price Determination Considering the Coordinated Operation of Hydrogen Fuel Cell Electric Vehicle, Power Network and Transportation Network. *IEEE Access* 2023; 11: 75508-21. 10.1109/ACCESS.2023.3296783.

[20] J. Wang et al. Charging Pricing for Autonomous Mobility-on-Demand Fleets Based on Game Theory. *Journal of Modern Power Systems and Clean Energy* 2024; 12(6): 2006-18. 10.35833/MPCE.2024.000139.

[21] Q. Gao, H. Li, K. Peng, C. Zhang, X. Qu. A real-time charging price strategy of distribution network based on comprehensive demand response of EVs and cooperative game. *Journal of Energy Storage* 2024; 101: 113805. 10.1016/j.est.2024.113805.

[22] M. Tostado-Véliz, X. Jin, R. Bhakar, F. Jurado. Coordinated pricing mechanism for parking clusters considering interval-guided uncertainty-aware strategies. *Applied Energy* 2024; 355: 122373. 10.1016/j.apenergy.2023.122373.

[23] X. Ge, G. Wang, R. Sun, F. Wang. A Distributed and Game-Theoretic-Based EV Charging Pricing Model Under Coupled Energy-Transportation-Information Networks. *IEEE Transactions on Smart Grid* 2025; 16(1): 652-64. 10.1109/TSG.2024.3460477.

[24] T. Qian, Z. Liang, C. Shao, Z. Guo, Q. Hu, Z. Wu. Unsupervised learning for efficiently distributing EVs charging loads and traffic flows in coupled power and transportation systems. *Applied Energy* 2025; 377(B): 124476. 10.1016/j.apenergy.2024.124476.

[25] R.A. Jabr. Distributionally Robust CVaR Constraints for Power Flow Optimization. *IEEE Transactions on Power Systems* 2020; 35(5): 3764-73. 10.1109/TPWRS.2020.2971684.

[26] A. Baringo, L. Baringo, J.M. Arroyo. Robust virtual power plant investment planning. *Sustainable Energy, Grids and Networks* 2023; 35: 101105. 10.1016/j.segan.2023.101105.

[27] S. Xie, Z. Hu, J. Wang. Two-stage robust optimization for expansion planning of active distribution systems coupled with urban transportation networks. *Applied Energy* 2020; 261: 114412. 10.1016/j.apenergy.2019.114412.

[28] N. Vespermann, T. Hamacher and J. Kazempour. Risk Trading in Energy Communities. *IEEE Transactions on Smart Grid* 2021; 12(2): 1249-63. 10.1109/TSG.2020.3030319.

[29] W. Hua, J. Jiang, H. Sun, F. Teng, G. Strbac. Consumer-centric decarbonization framework using Stackelberg game and Blockchain. *Applied Energy* 2022; 309: 118384. 10.1016/j.apenergy.2021.118384.

[30] C. Ruiz, A.J. Conejo. Robust transmission expansion planning. *European Journal of Operational Research* 2015; 242(2): 390-401. 10.1016/j.ejor.2014.10.030.

[31] X. Wang, F. Li, Q. Zhang, Q. Shi, J. Wang. Profit-Oriented BESS Siting and Sizing in Deregulated Distribution Systems. *IEEE Transactions on Smart Grid* 2023; 14(2): 1528-40. 10.1109/TSG.2022.3150768.

[32] M. Tostado-Véliz, S. Kamel, H.M. Hasanien, P. Arévalo, R.A. Turky, F. Jurado. A stochastic-interval model for optimal scheduling of PV-assisted multi-mode charging stations. *Energy* 2022; 253: 124219. 10.1016/j.energy.2022.124219.

[33] L.A. Roald, D. Pozo, A. Papavasiliou, D.K. Molzahn, J. Kazempour, A. Conejo. Power systems optimization under uncertainty: A review of methods and applications. *Electric Power Systems Research* 2023; 214(A): 108725. 10.1016/j.epsr.2022.108725.

[34] M. Tostado-Véliz, J.S. Giraldo, D.I. Álvarez, C. Cruz, F. Jurado. Robust day-ahead scheduling of cooperative energy communities considering multiple aggregators. *Sustainable Cities and Society* 2024; 116: 105878. 10.1016/j.scs.2024.105878.

[35] M. Tostado-Véliz, P. Arévalo, F. Jurado. An optimization framework for planning wayside and on-board hybrid storage systems for tramway applications. *Journal of Energy Storage* 2021; 43: 103207. 10.1016/j.est.2021.103207.

[36] I. Alsaidan, A. Khodaei, W. Gao. A Comprehensive Battery Energy Storage Optimal Sizing Model for Microgrid Applications. *IEEE Transactions on Power Systems* 2018; 33(4): 3968-80. 10.1109/TPWRS.2017.2769639.

[37] C. Ju, P. Wang, L. Goel, Y. Xu. A Two-Layer Energy Management System for Microgrids With Hybrid Energy Storage Considering Degradation Costs. *IEEE Transactions on Smart Grid* 2018; 9(6): 6047-57. 10.1109/TSG.2017.2703126.

[38] Y. Wan, J. Qin, Y. Shi, W. Fu, D. Zhang. Privacy-Preserving Operation Management of Battery Swapping and Charging System With Dual-Based Benders Decomposition. *IEEE Transactions on Smart Grid* 2023; 14(5): 3899-912. 10.1109/TSG.2023.3236329.

[39] A.A. Pesaran. Choices and Requirements of Batteries for EVs, HEVs, PHEVs. National Renewable Energy Laboratory 2011. NREL/PR-5400-51474. Online, available at: https://www.nrel.gov/docs/fy11osti/51474.pdf, (accessed 24 Mar. 2025).

[40] M.S. Javadi, M. Lotfi, A.E. Nezhad, A. Anvari-Moghaddam, J.M. Guerrero, J.P.S. Catalão. Optimal Operation of Energy Hubs Considering Uncertainties and Different Time Resolutions. *IEEE Transactions on Industry Applications* 2020; 56(5): 5543-52. 10.1109/TIA.2020.3000707.

[41] M. Tostado-Véliz, J.S. Giraldo, D.I. Álvarez, C. Cruz, F. Jurado. Robust day-ahead scheduling of cooperative energy communities considering multiple aggregators. *Sustainable Cities and Society* 2024; 116: 105878. 10.1016/j.scs.2024.105878.

[42] A.J. Conejo, C. Ruiz. Complementarity, Not Optimization, is the Language of Markets. *IEEE Open Access Journal of Power and Energy* 2020; 7: 344-53. 10.1109/OAJPE.2020.3029134.

[43] J. Fortuny-Amat, B. McCarl. A representation and economic interpretation of a two-level programming problem. *Journal of the Operational Research Society* 1981; 32(9): 783-92. 10.1057/jors.1981.156.

[44] T. Kleinert, M. Schmidt. Global optimization of multilevel electricity market models including network design and graph partitioning. Discrete Optimization 2019; 33: 43-69. 10.1016/j.disopt.2019.02.002.

[45] A.C. Davison, D.V. Hinkley. *Bootstrap Methods and their Application*. Part of: *Cambridge Series in Statistical and Probabilistic Mathematics*. Cambridge University Press, 1997. 9780521574716.

[46] Comisión Nacional de los Mercados y la Competencia. Precios Mercado. Online, available at: https://www.cnmc.es/estadistica/precios-mercado-2023, (accessed 12 Feb. 2025).

[47] D. Zhao, V. Dvorkin, S. Delikaraoglou, A.J.L.L., A. Botterud. Uncertainty-Informed Renewable Energy Scheduling: A Scalable Bilevel Framework. *IEEE Transactions on Energy Markets, Policy and Regulation* 2024; 2(1): 132-45. 10.1109/TEMPR.2023.3344126.

[48] GOE. From Charging to Sharing: What You Need to Know About V2G in 2025. Published 11 Feb. 2025. Online, available at: https://go-e.com/en/magazine/vehicle-to-grid, (accessed 27 Mar. 2025).

[49] A. Selim, S. Kamel, E.H. Houssein, F. Jurado, F.A. Hashim. A modified Runge–Kutta optimization for optimal photovoltaic and battery storage allocation under uncertainty and load variation. *Soft Computing* 2024; 28: 10369-89. 10.1007/s00500-024-09796-8.

[50] M. Tostado-Véliz, A.R. Jordehi, S.A. Mansouri, F. Jurado. A two-stage IGDT-stochastic model for optimal scheduling of energy communities with intelligent parking lots. *Energy* 2023; 263(D): 126018. 10.1016/j.energy.2022.126018.

[51] Gurobi Optimization L.L.C. Gurobi Optimizer Reference Manual. 2021. Online, available at: https://www.gurobi.com, (accessed 12 Feb. 2025).

[52] National Centers for Environmental Information. Land-based datasets and products. Online, available at: https://www.ncei.noaa.gov/products/land-based- station, (accessed 12 Feb. 2025).

[53] Electric Vehicle Database. Online, available at: https://www.ev-database.org, (accessed 12 Feb. 2025).

[54] M. Tostado-Véliz, A.R. Jordehi, Y. Zhou, S.A. Mansouri, F. Jurado. Best-case-aware planning of photovoltaic-battery systems for multi-mode charging stations. *Renewable Energy* 2024; 225: 120300. 10.1016/j.renene.2024.120300.

[55] L. Wei, Z. Luo, R. Baldacci, A. Lin. A New Branch-and-Price-and-Cut Algorithm for One-Dimensional Bin-Packing Problems. *Informs Journal on Computing* 2019; 32(2): 428-43. 10.1287/ijoc.2018.0867.

[56] Y. Li, B. Wang, Z. Yang, J. Li, C. Chen. Hierarchical stochastic scheduling of multi-community integrated energy systems in uncertain environments via Stackelberg game. *Applied Energy* 2022; 308: 118392. 10.1016/j.apenergy.2021.118392.